NATIONAL ADVISORY COMMITTEE FOR AERONAUTICS

TECHNICAL NOTE 2123

INVESTIGATION OF TURBULENT FLOW IN A TWO-DIMENSIONAL CHANNEL

By John Laufer

California Institute of Technology

Washington
July 1950

NATIONAL ADVISORY COMMITTEE FOR AERONAUTICS

TECHNICAL NOTE 2123

INVESTIGATION OF TURBULENT FLOW IN A TWO-DIMENSIONAL CHANNEL

By John Laufer

SUMMARY

A detailed exploration of the field of mean and fluctuating quantities in a two-dimensional turbulent channel flow is presented. The measurements were repeated at three Reynolds numbers, 12,300, 30,800, and 61,600, based on the half width of the channel and the maximum mean velocity. A channel of 5-inch width and 12:1 aspect ratio was used for the investigation.

Mean-speed and axial-fluctuation measurements were made well within the laminar sublayer. The semitheoretical predictions concerning the extent of the laminar sublayer were confirmed. The distribution of the velocity fluctuations in the direction of mean flow u' shows that the influence of the viscosity extends farther from the wall than indicated by the mean velocity profile, the region of influence being approximately four times as wide.

Fluctuations perpendicular to the flow in the lateral and vertical directions v' and w', respectively, and the correlation coefficient $k = \dfrac{\overline{u'v'}}{\sqrt{\overline{u'^2}}\sqrt{\overline{v'^2}}}$ were also measured. The turbulent shearing stress was computed by three different methods. The results show satisfactory agreement for the two lower Reynolds numbers. In the case of the highest Reynolds number, however, the total shearing stress τ obtained from the fluctuation measurements was approximately 20 percent lower than that computed from the mean-velocity and mean-pressure measurements. All dimensionless mean fluctuating quantities were found to decrease with increasing Reynolds number. Measurements of the scales of turbulence L_y and L_z and microscales of turbulence λ_y and λ_z across the channel are presented and their variation with Reynolds number is discussed. Using a new technique, values for the microscale λ_x were obtained; a new method for estimating the scale L_x is also given.

The energy balance in the turbulent flow field was calculated from the measured quantities. From this calculation it is possible to give a descriptive picture of turbulent-energy diffusion in the center portion of the channel cross section.

For the flow corresponding to a Reynolds number of 30,800 the energy spectrum of the $\overline{u'^2}$-fluctuations at various points across the channel, including one in the laminar sublayer, was obtained.

At station $\frac{y}{d} = 0.4$, where y is lateral distance and d is half width of the channel, the contribution to the turbulent shear stress from various frequency bands was measured and it was found that the contribution corresponding to frequencies above 1500 cycles per second is negligible. Since the spectrum of $\overline{u'^2}$ at this point extends to about 5000 cycles per second it is evident that the high frequencies are nearly isotropic in agreement with Kolmogoroff's hypothesis.

INTRODUCTION

In recent years a considerable step forward was made in the theory of turbulence. Kolmogoroff (reference 1), Heisenberg (reference 2), and Onsager (reference 3) obtained independently an energy-spectrum law that holds in rather restricted types of turbulent flows. This progress gave a new impetus to both theoretical and experimental investigations. The experimental worker may follow two principal methods of approach to the problem. First, he may establish flow fields which satisfy sufficiently the assumptions of the new theory, namely, that the flow is isotropic and of high Reynolds number so that the influence of viscosity is a minimum and the effect of the turbulence-producing mechanism is small. Under these conditions he may measure quantities such as correlation functions, scales, and microscales that are defined exactly in the flow field and may compare his results with those predicted by the theory. The main difficulty with this method is to predict how closely one has to approximate in the actual flow the conditions assumed in the theory. In other words, the sensitivity of the theory to deviations from true isotropic conditions is not known and in case the measurements do not agree with the theory one does not know whether to attribute the disagreement to faulty assumptions in the theory or to the incomplete isotropic conditions of the flow. Furthermore, the imposition of the condition of isotropy to fluctuating fields may be a very strong restriction and the study of such fields may not yield the complete picture of the turbulence mechanism.

The second method of approach is to establish a simple nonisotropic turbulent flow field with well-defined boundary conditions and, in the light of the existing theories, to try to obtain information on the mechanism of energy transfer from the low frequencies of the energy spectrum to the high ones. The present investigation of a turbulent channel flow has this purpose in mind in its long-range program.

The difficulties of this method are immediately realized. Because of the nonisotropic nature of the flow, characteristic quantities such as scale and microscale are no longer well defined and it is very possible that in the first stages of the investigation certain quantities will be measured that later will prove to be trivial. On the other hand, the main advantage of a fully developed channel flow is the fact that, in contrast with the flow behind grids, flow conditions are steady; no decay of mean or fluctuating quantities exists in the direction of the flow. Consequently, the turbulent energy goes through all of its stages of transformation across the channel section — turbulent-energy production from the mean flow, energy diffusion, and turbulent and laminar dissipation — and one may study these transformations in detail.

It has become clear that the phenomenological theories of turbulence, such as the mixing-length theories, have lost most of their importance. These theories, developed in the late twenties and early thirties, were aimed specifically at an evaluation of the mean-velocity distribution in turbulent flow. The existing experimental evidence shows clearly that the mean-velocity distribution is very insensitive to the essential assumptions introduced into the phenomenological theories. In fact, purely dimensional arguments generally suffice to give the shape of the mean velocity profile with sufficient accuracy. For the further development of an understanding of turbulence, detailed measurements of the field of fluctuating rather than of mean velocities are necessary. The program of experimental research of which this work is one part is based on this reasoning. It is quite apparent and natural that the same conclusions have been drawn by workers in the turbulent field elsewhere and that, in general, the main emphasis of current experimental investigation is the exploration of the field of the fluctuating-velocity components.

The present set of experiments deals with flow in a two-dimensional channel, that is, with pressure flow between two flat walls. Channel flow of this type is the simplest type of turbulent flow near solid boundaries which can be produced experimentally. The simpler Couette type flow requires that one wall move with constant velocity, a condition which is difficult to realize experimentally. It can be approximated by the flow between concentric cylinders, but complications due to centrifugal forces arise here. The simple geometry of a

two-dimensional channel allows an integration of the Reynolds equations, and the turbulent shearing stress can then be related directly to the shearing stress on the surfaces which, in turn, can be determined from the mean-pressure gradient or the slope of mean velocity profile at the wall.

The relation between the apparent stresses and the wall shearing stress can be used to advantage in two fashions. It is here possible to obtain the magnitude of the correlation coefficient responsible for the apparent shear by measuring only the intensities of the turbulent fluctuations. The turbulent shearing stress can also be measured directly by means of the hot-wire anemometer. A comparison with the shear distribution obtained from mean-pressure-gradient or mean-velocity-profile measurements serves then as a very useful check on the underlying assumptions, on the one hand, and specifically as a check on the reliability and accuracy of the direct measurements, on the other.

Measurements of channel flow have previously been made by Doench (reference 4), Nikuradse (reference 5), Wattendorf and Kuethe (references 6 and 7), and Reichardt (references 8 and 9). A few unpublished measurements have been made recently at the Polytechnic Institute of Brooklyn.

Doench's and Nikuradse's measurements were concerned only with the mean-velocity distribution and are thus of not too much interest for a comparison with the present set of measurements. Wattendorf measured the intensity of the fluctuating-velocity components and then deduced the correlation coefficient from the mean-pressure measurements. The technique for measuring the axial component of the velocity fluctuation was well developed at the time, but the cross component was only tentatively measured.

The most complete set of measurements is due to the work of Reichardt, who measured velocity fluctuations in the direction of the flow and normal to the wall as well as the turbulent shear directly. Reichardt found very good agreement between the shearing stress determined in these two ways; his paper comes closest to the present investigation and his results will be used for comparison. The Reynolds number in Reichardt's measurements was 8000, which is lower than the range covered by the present measurements. A criticism which can be made of Reichardt's investigation is his use of a tunnel of only 1:4 aspect ratio. The two-dimensional character of the flow is thus somewhat doubtful. Wattendorf's experiments were made in a channel of very large aspect ratio (18:1) and are thus free of this criticism.

In a preliminary investigation a channel 1 inch wide and 60 inches high was chosen. The measurements, however, have shown that in this

case the scale of turbulence is so small that great care must be taken to correct the hot-wire readings for the effect of wire length. Measurements of the microscales were, in fact, impossible in the 1-inch channel. The microscales were about 0.1 centimeter and thus smaller than the length of the wire. The corrections for the case of measurements of v' and w' were about 30 percent. Since the method of correction becomes very inaccurate for such large ratios of wire length to microscale, the measurements were repeated in a 5-inch channel with a 12:1 aspect ratio. This ratio was still large enough to insure two-dimensional flow and the length corrections were greatly reduced.

This investigation was conducted at the Guggenheim Aeronautical Laboratory, California Institute of Technology, under the sponsorship and with the financial assistance of the National Advisory Committee for Aeronautics.

The author wishes to acknowledge the constant advice and help in both experimental methods and interpretation of results of Dr. H. W. Liepmann during this investigation. He also wishes to thank Dr. C. B. Millikan for his continuous interest in this research. The cooperation of Dr. F. E. Marble and Mr. F. K. Chuang is much appreciated.

SYMBOLS

x	longitudinal coordinate in direction of flow; $x = 0$ corresponds to channel exit
y	lateral coordinate; $y = 0$ corresponds to channel wall
z	vertical coordinate
d	half width of channel (2.5 in.)
δ	thickness of laminar sublayer
u	mean velocity at any point in channel
U_o	maximum value of mean velocity
u'	instantaneous value of velocity fluctuations in direction of mean flow x
v', w'	instantaneous values of velocity fluctuations normal to mean flow in directions y and z, respectively

$\tilde{u}'$ root-mean-square value of velocity fluctuations in direction of mean flow x

$\tilde{v}', \tilde{w}'$ root-mean-square values of velocity fluctuations normal to mean flow in directions y and z, respectively

p pressure at any point in channel

ρ air density

τ total shearing stress

τ_o shearing stress at wall

U_τ friction velocity $\left(\sqrt{\tau_o/\rho}\right)$

μ absolute viscosity of air

ν kinematic viscosity

R Reynolds number based on half width of channel and maximum mean velocity

k correlation coefficient responsible for apparent shear $\left(\dfrac{\overline{u'v'}}{\sqrt{\overline{u'^2}}\sqrt{\overline{v'^2}}}\right)$

R_x, R_y, R_z correlation coefficients as functions of X, Y, and Z, respectively

$\lambda_x, \lambda_y, \lambda_z$ microscales of turbulence

$$\left(\frac{\overline{u'^2}}{\lambda_x^2} \equiv \overline{\left(\frac{\partial u'}{\partial x}\right)^2},\quad \frac{\overline{u'^2}}{\lambda_y^2} \equiv \frac{1}{2}\overline{\left(\frac{\partial u'}{\partial y}\right)^2},\quad \frac{\overline{u'^2}}{\lambda_z^2} \equiv \frac{1}{2}\overline{\left(\frac{\partial u'}{\partial z}\right)^2}\right)$$

L_x, L_y, L_z scales of turbulence

$$\left(L_x \equiv \int_0^\infty R_x \, dX, \quad L_y \equiv \int_0^\infty R_y \, dY, \quad L_z \equiv \int_0^\infty R_z \, dZ \right)$$

X, Y, Z distances (in the x–, y–, and z–direction, respectively) between points at which correlation fluctuations are measured

σ ratio of square of compensated and uncompensated fluctuations

M time constant expressing thermal lag of hot–wire

n frequency, cycles per second

$F_{\overline{u'^2}}(n), F(n)$ fraction of turbulent energy $\overline{u'^2}$ associated with band width dn

$F_{\overline{u'v'}}(n)$ fraction of turbulent shear $\overline{u'v'}$ associated with band width dn

W dissipation of turbulent energy

t time

e_1, e_2 voltage fluctuations

ANALYTICAL CONSIDERATIONS

Equations of Motion for Two–Dimensional Channel Flow

The mean– and fluctuating–velocity components are denoted by u_i and u_i', respectively; Cartesian coordinates are designated by x_i; and p_{ik} denotes the components of the stress tensor which includes both the viscous and apparent (Reynolds) stresses. The Reynolds equation and the continuity equation for steady flow can thus be written, using Cartesian tensor notation,

$$\rho u_k \frac{\partial u_i}{\partial x_k} = \frac{\partial p_{ik}}{\partial x_k} \tag{1a}$$

$$\frac{\partial u_i}{\partial x_i} = 0 \tag{1b}$$

where

$$p_{ik} = \begin{vmatrix} -p + 2\mu \dfrac{\partial u_1}{\partial x_1} - \rho\overline{u_1'^2} & \mu\left(\dfrac{\partial u_1}{\partial x_2} + \dfrac{\partial u_2}{\partial x_1}\right) - \rho\overline{u_1'u_2'} & \mu\left(\dfrac{\partial u_1}{\partial x_3} + \dfrac{\partial u_3}{\partial x_1}\right) - \rho\overline{u_1'u_3'} \\ \mu\left(\dfrac{\partial u_1}{\partial x_2} + \dfrac{\partial u_2}{\partial x_1}\right) - \rho\overline{u_1'u_2'} & -p + 2\mu \dfrac{\partial u_2}{\partial x_2} - \rho\overline{u_2'^2} & \mu\left(\dfrac{\partial u_2}{\partial x_3} + \dfrac{\partial u_3}{\partial x_2}\right) - \rho\overline{u_2'u_3'} \\ \mu\left(\dfrac{\partial u_1}{\partial x_3} + \dfrac{\partial u_3}{\partial x_1}\right) - \rho\overline{u_1'u_3'} & \mu\left(\dfrac{\partial u_2}{\partial x_3} + \dfrac{\partial u_3}{\partial x_2}\right) - \rho\overline{u_2'u_3'} & -p + 2\mu \dfrac{\partial u_3}{\partial x_3} - \rho\overline{u_3'^2} \end{vmatrix}$$

For channel flow between two parallel flat walls,

$$u_1 = u(y)$$

$$u_2 = 0$$

$$u_3 = 0$$

$$p_{ik} = \begin{vmatrix} -p - \rho\overline{u'^2} & \mu \dfrac{du}{dy} - \rho\overline{u'v'} & 0 \\ \mu \dfrac{du}{dy} - \rho\overline{u'v'} & -p - \rho\overline{v'^2} & 0 \\ 0 & 0 & -p - \rho\overline{w'^2} \end{vmatrix}$$

where x, y, and z replace x_i, and u', v', and w' replace u_i' for convenience in writing the now much simpler equations. Equation (1b) is thus automatically satisfied and equation (1a) becomes:

$$\left.\begin{aligned} 0 &= \frac{\partial}{\partial x}\left(-p - \rho\overline{u'^2}\right) + \frac{\partial}{\partial y}\left(\mu\frac{du}{dy} - \rho\overline{u'v'}\right) \\ 0 &= \frac{\partial}{\partial y}\left(-p - \rho\overline{v'^2}\right) + \frac{\partial}{\partial x}\left(\mu\frac{du}{dy} - \rho\overline{u'v'}\right) \end{aligned}\right\} \tag{2}$$

In fully developed turbulent flow the variation of mean values of the fluctuating quantities with x should be zero; that is, the flow pattern is independent of the streamwise direction. Hence, equations (2) become:

$$\frac{1}{\rho}\frac{\partial p}{\partial x} = \nu\frac{d^2u}{dy^2} - \frac{d\overline{u'v'}}{dy}$$

or

$$\frac{1}{\rho}\frac{\partial p}{\partial x} = \frac{1}{\rho}\frac{d\tau}{dy} \tag{3a}$$

$$\frac{1}{\rho}\frac{\partial p}{\partial y} = -\frac{\partial\overline{v'^2}}{\partial y} \tag{3b}$$

Differentiating equation (3b) with respect to x gives $\frac{1}{\rho}\frac{\partial^2 p}{\partial x\partial y} = 0$; consequently $\partial p/\partial x$ is independent of y and equation (3a) is immediately integrable. Thus

$$\frac{y}{\rho}\frac{\partial p}{\partial x} = \nu\frac{du}{dy} - \overline{u'v'} + \text{Constant}$$

In the center of the channel the shear vanishes; hence if the channel has the width 2d,

$$\text{Constant} = \frac{d}{\rho}\frac{\partial p}{\partial x}$$

and hence

$$\frac{1}{\rho}\frac{\partial p}{\partial x}(y - d) = \nu\frac{du}{dy} - \overline{u'v'}$$

Or in nondimensional form:

$$\frac{y - d}{\rho U_o^2}\frac{\partial p}{\partial x} = \frac{\nu}{U_o^2}\frac{du}{dy} - \frac{\overline{u'v'}}{U_o^2} \tag{4}$$

In terms of the shearing stress at the wall,

$$-\frac{\tau_o}{\rho U_o^2}\frac{y - d}{d} = \frac{\nu}{U_o^2}\frac{du}{dy} - \frac{\overline{u'v'}}{U_o^2} \tag{5}$$

It is evident from equations (4) and (5) that τ_o can be determined in three different ways:

(a) From the mean-pressure gradient

$$\tau_o = -d\frac{\partial p}{\partial x}$$

(b) From the slope of the mean velocity profile near the wall

$$\tau_o = \mu\left(\frac{du}{dy}\right)_{y=0}$$

(c) From a direct measurement of $\overline{u'v'}$

$$\tau_o = \left(\rho\overline{u'v'} - \mu\frac{du}{dy}\right)\frac{d}{y - d}$$

since if y/d is not too small,

$$\mu \frac{du}{dy} \ll \rho\overline{u'v'}$$

and item (c) becomes

$$\tau_o = \rho\overline{u'v'} \frac{d}{y - d}$$

The technically simplest way to determine τ_o, and thus in fact the complete shear distribution, is a measurement of $\partial p/\partial x$. This is the method applied in most investigations.

To determine the slope of the velocity profile near the wall, the profile has to be known up to points very close to the wall, that is, at least to distances $\frac{y}{d} = 10^{-2}$. This in general requires the use of the hot-wire anemometer and very precise measurements.

The third method requires a direct measurement of the correlation between the axial and lateral velocity fluctuations. The technique of this type of measurement is known and was first applied by Reichardt and by Skramstad and, in somewhat different form, in recent investigations at the National Bureau of Standards, Polytechnic Institute of Brooklyn, and California Institute of Technology.

In the present investigation all three methods have been applied and the results compared, with the exception of the flow at the lowest Reynolds number. In this case the pressure gradient is extremely small (approx. 0.0003 mm of alcohol/cm) and reasonably accurate measurements were not possible. This comparison of the three methods has the advantage that it gives a good indication of the absolute accuracy of measurements of the fluctuating quantities and the correlation coefficient k.

Energy Equation

Writing equation (1a) in the form

$$\rho u_k \frac{\partial u_i}{\partial x_k} = -\frac{\partial p}{\partial x_i} + \mu \nabla^2 u_i \qquad (6)$$

and multiplying it by u_i, the following relation is obtained:

$$\frac{1}{2}\rho\frac{\partial u_i u_i u_k}{\partial x_k} = -\frac{\partial p u_i}{\partial x_i} + \mu u_i \frac{\partial^2 u_j}{\partial x_j \partial x_j}$$

Transforming the last term by partial integration the energy equation of the mean flow becomes

$$\frac{1}{2}\rho\frac{\partial u_i u_i u_k}{\partial x_k} = -\frac{\partial p u_i}{\partial x_i} + \frac{1}{2}\mu\frac{\partial^2 u_i u_i}{\partial x_j \partial x_j} - \mu\left(\frac{\partial u_i}{\partial x_j}\right)\left(\frac{\partial u_i}{\partial x_j}\right) \tag{7}$$

The velocity perturbations can now be introduced:

$$u_1 = u + u'$$

$$u_2 = v'$$

$$u_3 = w'$$

Since the velocities are independent of the coordinates x and z the following equation is obtained after averaging:

$$\rho\overline{u'v'}\frac{du}{dy} + \rho u\frac{\overline{du'v'}}{dy} + \frac{1}{2}\rho\frac{d}{dy}\overline{v'\left(u'^2 + v'^2 + w'^2\right)} = -u\frac{\partial p}{\partial x} - \frac{\overline{\partial v' p}}{\partial y} +$$

$$\mu u\frac{d^2u}{dy^2} + \frac{1}{2}\mu\frac{d^2}{dy^2}\overline{\left(u'^2 + v'^2 + w'^2\right)} - \mu\overline{\left(\frac{\partial u_i'}{\partial x_j}\right)\left(\frac{\partial u_i'}{\partial x_j}\right)}$$

Making use of equation (3a) this simplifies to

$$\tau\frac{du}{dy} = \frac{d}{dy}\left[\overline{\rho v'\left(\frac{u'^2 + v'^2 + w'^2}{2}\right) + v'p}\right] + \mu\left(\frac{du}{dy}\right)^2 - \frac{1}{2}\mu\frac{d^2}{dy^2}\overline{\left(u'^2 + v'^2 + w'^2\right)}$$

$$\mu\overline{\left(\frac{\partial u_i'}{\partial x_j}\right)\left(\frac{\partial u_i'}{\partial x_j}\right)}$$

This form was obtained by Von Kármán (reference 10) while discussing a nonisotropic flow in terms of the statistical theory of turbulence. In order to see the relative orders of magnitudes of the different terms in the equation, Von Kármán expresses them in terms of a single velocity $q = \sqrt{\overline{u'^2 + v'^2 + w'^2}}$ and a characteristic length D corresponding to the width of the channel. Since

$$\frac{\tau}{\rho} \approx -\overline{u'v'} = O(q^2)$$

and

$$\frac{du}{dy} = O\left(\frac{\sqrt{\frac{\tau}{\rho}}}{D}\right) = O\left(\frac{q}{D}\right)$$

the above equation may be written as

$$A_1 \frac{q^3}{D} = A_2 \frac{q^3}{D} + A_3 \frac{\nu q^2}{D^2} + A_4 \frac{\nu q^2}{D^2} + A_5 \frac{\nu q^2}{\lambda^2}$$

where the coefficients have the characteristics of correlation functions and λ is the microscale of turbulence. For a high Reynolds number flow $\frac{qD}{\nu} \gg 1$, it follows that $\frac{\nu q^2}{D^2} \ll \frac{q^3}{D}$. Thus the second and third term on the right side of the equation may be neglected. Since the pertinent quantities have been measured during the present work, the order of magnitude of these terms can be directly evaluated and the omission of the terms is found to be justified. The above equation thus contains only terms of the forms q^3/D and $\nu q^2/\lambda^2$; these terms should be of the same order of magnitude and therefore $\frac{q\lambda^2}{\nu D} = O(1)$. It is of considerable interest to see whether experimental results confirm this relation. Taking as an example results from the measurements at $R = 30{,}800$ and $\frac{y}{d} = 0.5$ $\left(\text{where } \frac{q^3}{D} \approx 11 \times 10^3 \text{ and } \frac{\nu q^2}{\lambda^2} \approx 1.7 \times 10^3\right)$

$$q = 52 \text{ centimeters per second}$$

$$\lambda_y = 0.5 \text{ centimeter}$$

therefore

$$\frac{q\lambda^2}{\nu D} = \frac{52 \times 0.25}{0.155 \times 12.7} = 6.6$$

This ratio seems to be fairly constant for different Reynolds numbers and across the channel cross section.

In view of the above dimensional considerations, the energy equation may be written

$$\tau \frac{du}{dy} = \frac{d}{dy}\left(\overline{\rho v' \frac{u'^2 + v'^2 + w'^2}{2}} + \overline{v'p}\right) + \mu\overline{\left(\frac{\partial u_i'}{\partial x_j}\right)\left(\frac{\partial u_i'}{\partial x_j}\right)} \qquad (8)$$

The equation expresses the fact that the energy produced by the turbulent shear forces at a certain point is partly diffused and partly dissipated. This equation has been used in estimating the energy diffusion across the channel, since from the measured quantities the production term and dissipation can be calculated.

EQUIPMENT AND PROCEDURE

Wind Tunnel

The investigation was carried out in the wind tunnel shown in figure 1. The turbulence level is controlled by a honeycomb and seamless precision screens, followed by an approximately 29:1 contraction. The screens have 18 meshes per inch and a wire diameter of 0.018 inch. The honeycomb consists of paper mailing tubes, 6 inches long and 1 inch in diameter.

The over-all length of the channel is 23 feet. At the entrance section it is 3 inches wide and has an aspect ratio of 20:1. In a distance of 7 feet it expands to a width of 5 inches and the aspect ratio is reduced to 12:1. The walls of the exit portion of the channel (about 6 ft) are made of $\frac{3}{4}$-inch-thick plywood with a $\frac{1}{4}$-inch birch inside cover. They were specially treated in order to acquire a smooth finish and were reinforced in order to avoid warping (fig. 2); in spite of this a few percent of width variation existed.

The tunnel is operated by a 62-horsepower stationary natural-gas engine — normally operating at a fraction of its rating — which drives two eight-bladed fans. The speed is remotely controlled by means of a small electric motor which drives the throttle through a gear and lead-screw system.

The experiments were carried out at speeds of 3, 7.5, and 15 meters per second.

Traversing Mechanism

Figure 3 shows the type of traversing mechanism used during the experiments. It consists simply of a micrometer screw on which the hot-wire support is fastened. The support can rotate freely in a plane perpendicular to the air flow; thus, the hot-wire may be adjusted exactly parallel to the wall.

The zero reading of the traversing mechanism ($y = 0$) was carefully found using the following method: The hot-wire was placed close to the wall (approx. 0.025 cm away); the distance between the wire and its image in the polished wall was measured by means of an ocular micrometer. The position of the wire is, of course, one-half of the observed distance and could be determined with an accuracy of ± 0.0005 centimeter.

In order to obtain the pressure distribution along the middle of the channel a 6-inch-long thin-walled tube 3/8 inch in diameter was used with a small static-pressure hole drilled close to its end. The tube was free to slide in a support at the entrance of the channel so that the position of the pressure hole relative to the channel exit could be changed. The tube was kept straight and under tension by means of weights.

Hot-Wire Equipment

All velocity measurements were made with hot-wire anemometers. The frequency response of the amplifier-compensator unit of the hot-wire equipment, using a 0.00024-inch wire at standard operating conditions, is flat from approximately 2 to 10,000 cycles per second.

The compensation of the hot-wire for thermal lag is accomplished by a capacity network. The range of time constants was chosen from 0 to 1 millisecond corresponding to the characteristics of 0.00005- to 0.00024-inch wires at the operating conditions employed in general at GALCIT. No attempt was made to extend the range of compensation to larger values of M, since in this case the noise level soon becomes appreciable.

The correct setting of the compensating unit was found using the square-wave method described by Kovásznay (reference 11). The time constants of the wires used for turbulence measurements fell between 0.1 and 0.9 millisecond.

The output readings were taken with a thermocouple and precision potentiometer.

Mean-speed measurements.— A $\frac{1}{2}$-mil (0.0005-in.) platinum wire of 1-centimeter length was used to measure the mean speed. The measurements were made by the constant-resistance method. This method has the advantage of keeping the wire temperature constant through the velocity field.

Turbulence measurements.— For the investigation of turbulent fluctuations, 0.00024-inch Wollaston wire was used. The wire was soft-soldered to the tips of fine sewing needles after the silver coating had been etched off. The two lateral components v' and w' and the correlation coefficient $k = \frac{\overline{u'v'}}{\sqrt{\overline{u'^2}}\sqrt{\overline{v'^2}}}$ were measured using the X-wire technique. The method was essentially the same as described in detail in previous reports from this laboratory. (See, for example, reference 12.)

The X-meters for shear measurements had angles between the wires of approximately 90°. The angles of the v',w'-meter were of the order of 30°. The wire length of the u'-meter was about 1.5 millimeters and that of the v'-meter was 3 millimeters.

The parallel-wire technique used recently at the Polytechnic Institute of Brooklyn was also tried in order to obtain the lateral component of the velocity fluctuation and the shear close to the wall. The parallel-wire instrument is superior to the X-meter since it allows an exploration of the turbulent field up to distances of a few thousandths of an inch from the wall. However, it was found impossible to obtain reliable values with this instrument. The corrections due to u'-fluctuations and to unequal heating of the wires were pronounced and not easily accountable. The method was therefore temporarily abandoned after considerable time and labor had been spent on it.

Measurements of correlations between two points.— The correlation functions between values of u' at points along the y- and z-axis, that is,

$$R_y = \frac{\overline{u'(0)u'(Y)}}{\sqrt{\overline{u'(0)^2}}\sqrt{\overline{u'(Y)^2}}}$$

$$R_z = \frac{\overline{u'(0)u'(Z)}}{\overline{u'^2}}$$

were measured using the standard technique (reference 12). The scales of turbulence L_y and L_z and the microscales λ_y and λ_z at different points across the channel were obtained from these measurements.

Measurements of λ_x.— A method suggested by Townsend (reference 13) was applied to measure λ_x. Using an electronic differentiation circuit the amplifier output signal was differentiated and λ_x computed from the following relation:

$$\overline{\left(\frac{\partial u'}{\partial t}\right)^2} = u^2 \overline{\left(\frac{\partial u'}{\partial x}\right)^2} = u^2 \frac{\overline{u'^2}}{\lambda_x^2}$$

The error involved in the approximation $\frac{\partial}{\partial t} \longrightarrow u \frac{\partial}{\partial x}$ can be estimated and it may be seen that the above relation holds with reasonable accuracy over the large center portion of the channel.

A new technique for the measurement of λ_x has also been applied. The method is described in detail in reference 14 and consists in counting the zeros of an oscillograph trace of the u'-fluctuations. From these counts λ_x may be calculated directly by assuming a normal and independent distribution for both u' and $\partial u'/\partial x$:

$$\frac{1}{\lambda_x} = \frac{\pi}{U_o} \times \text{Average number of zeros of } u' \text{ per second}$$

It is known that the distribution of u' is closely a Gaussian one even in nonistropic turbulence (see, for instance, reference 15); however, for the case of $\partial u'/\partial x$ a small deviation from the normal distribution was found (reference 13). For the preliminary measurements of λ_x reported presently, no corrections were applied as yet for this effect. Figure 4 shows an oscillograph trace of the u'-fluctuation in the middle of the channel at $R = 30{,}800$. The trace represents an interval of approximately 1/20 second.

Measurement of L_x.— The following simple procedure[1] was applied to obtain a rough estimate of scale of turbulence corresponding to correlations between points along the x-axis: Denote by $F(n)$ the

[1]This method was suggested by Dr. H. W. Liepmann.

fraction of turbulent intensity which is contributed by frequencies between n and $n + dn$; that is,

$$\overline{u'(n)^2}\, dn = \overline{u'^2} F(n)\, dn$$

and thus

$$\int_0^\infty F(n)\, dn = 1$$

Consider now an uncompensated hot-wire. If the time constant of this uncompensated wire is M, the response will be

$$\left[\overline{u'(n)^2}\right]_{\text{uncomp.}}$$

where

$$\left[\overline{u'(n)^2}\right]_{\text{uncomp.}} = \frac{\overline{u'(n)^2}}{1 + M^2n^2}$$

The total intensity for the uncompensated wire will then be given by[2]

$$\left(\overline{u'^2}\right)_{\text{uncomp.}} = \overline{u'^2} \int_0^\infty \frac{F(n)\, dn}{1 + M^2n^2}$$

Thus, if the ratio of the response of the same wire compensated and uncompensated is denoted by σ,

$$\frac{1}{\sigma} = \int_0^\infty \frac{F(n)}{1 + M^2n^2}\, dn \tag{9}$$

In order to estimate L_x, $F(n)$ is assumed to have the simple form

$$F(n) = \frac{2}{\pi} \frac{\frac{L_x}{U_o}}{1 + n^2 \frac{L_x^2}{U_o^2}}$$

---

[2]Formulas of this general type have been proposed by Kampé de Feriet and by Frenkiel for determining the spectrum of turbulence from uncompensated hot-wire measurements by varying M (reference 16).

which was given by Dryden (reference 17) and corresponds to an experimental correlation curve.

Then

$$\frac{1}{\sigma} = \frac{2}{\pi} \int_0^\infty \frac{\frac{L_x}{U_o}}{\left(1 + n^2 \frac{L_x^2}{U_o^2}\right)\left(1 + M^2 n^2\right)} dn$$

or with

$$\eta = \frac{L_x n}{U_o}$$

$$\alpha = \frac{M U_o}{L_x}$$

then

$$\frac{1}{\sigma} = \frac{2}{\pi} \int_0^\infty \frac{d\eta}{\left(1 + \eta^2\right)\left(1 + \alpha^2 \eta^2\right)} = \frac{1}{1 + \alpha}$$

Hence

$$L_x = \frac{M U_o}{\sigma - 1}$$

Thus by measuring the ratio of the mean squares of the fluctuating velocities with and without compensation, L_x can be estimated.

The procedure was checked in the flow behind a $\frac{1}{2}$-inch grid where the lateral scale was measured and where because of isotropy the relation $L_x = 2L_y$ should hold fairly well.

The results were:

$$\sigma = 1.85$$

$$M = 7 \times 10^{-4} \text{ second}$$

$$U_o = 1.5 \times 10^3 \text{ centimeters per second}$$

therefore

$$L_x = 1.24 \text{ centimeters}$$

Direct measurements gave $L_y = 0.553$ centimeter. Hence $L_x = 1.11$ centimeters which shows that this method of estimating the value of L_x is satisfactory.

Measurement of turbulent-energy spectrum.- In order to be able to measure accurately the energy distribution over a wide frequency band, it was found necessary to use extremely thin wires with small time constants and thus to increase the signal-to-noise ratio. Wires of 0.00005-inch diameter, operating with time constants of approximately 2×10^{-4} second, were used. In this way it was possible to detect energy values in the high-frequency bands that were 10^{-7} times the value corresponding to zero frequency.

The hot-wire signal was fed into a Hewlett-Packard wave analyzer, the output circuit of which was somewhat altered in order to be able to feed the output signal into a root-mean-square voltmeter. The averaging characteristics of the root-mean-square meter were checked and, for a narrow-band-width signal, were found to give the same mean values as those calculated from thermocouple readings.

With this method the energy of the $\overline{u'^2}$-fluctuation was measured at different points across the channel. At $\frac{y}{d} = 0.4$ the spectrum of the turbulent shear $\overline{u'v'}$ was also obtained.[3] An X-type meter was used, both wires making an angle of 45° with the free-stream direction. If $\overline{e_1^2}$ and $\overline{e_2^2}$ are the mean-square voltage fluctuations (corrected for time lag) across the two wires it may be shown (reference 12) that

$$\overline{e_1^2} - \overline{e_2^2} = \text{Constant} \times \overline{u'v'}$$

If e_1 and e_2 are fed into the wave analyzer then the above relation holds for all band widths dn; that is,

$$\overline{e_1(n)^2} - \overline{e_2(n)^2} = \text{Constant} \times \overline{u'v'(n)}$$

---

[3]This method appears to have been first used by Dr. Stanley Corrsin in a turbulent jet (private communication).

PRELIMINARY MEASUREMENTS IN A 1-INCH CHANNEL

In the initial stages of the turbulent-channel-flow investigation a two-dimensional channel of 1-inch width was used. Measurements of mean and fluctuating velocities and of the correlation coefficient k were completed. The scales L_y and L_z were also measured at the channel center and were found to be about 0.2 to 0.3 centimeter. This small-scale turbulence existing in the channel imposed a definite limitation on the accuracy of the fluctuating measurements. Wire-length corrections as high as 30 percent had to be applied to the measurements of v' and w'. Furthermore, no microscales could be measured accurately; thus one of the objectives of the investigation, the calculation of the energy dissipation across the channel, could not be obtained. Nevertheless, results show good consistency; the three independent measurements of the turbulent shear indicate satisfactory agreement.

It is of interest to present these preliminary measurements, the Reynolds number of which was 12,200, and to compare them with those obtained in the 5-inch channel. Figure 5 shows the distribution of all the measured quantities in the 1-inch channel and it may be directly compared with figure 16 which shows the quantities measured in the 5-inch channel at nearly the same Reynolds number.

Although the slopes of the mean velocities at the wall are almost the same in each case $\left(\text{for the 1-inch channel } \frac{\tau_o}{\rho U_o^2} = 0.0019\text{; for the 5-inch channel } \frac{\tau_o}{\rho U_o^2} = 0.0018\right)$, the velocity ratios u/U_o in the 5-inch channel seem to be lower across most of the channel. This indicates that a more intense turbulent-energy production $\tau\frac{du}{dy}$ takes place in the 5-inch channel. Indeed, the turbulent-velocity fluctuations $\tilde{u}'/U_o$, $\tilde{v}'/U_o$, and $\tilde{w}'/U_o$ (especially $\tilde{u}'/U_o$) increase at a faster rate toward the wall in the wider channel, although their values at the channel center check very well in the two cases. The shear distribution $\tau/\rho U_o^2$ is almost the same for the two channels; it follows, therefore, from the relation

$$\frac{\overline{u'v'}}{U_o^2} = k\,\frac{\tilde{u}'}{U_o}\,\frac{\tilde{v}'}{U_o}$$

that k must have a higher absolute value in the 1-inch channel since both $\tilde{u}'/U_o$ and $\tilde{v}'/U_o$ are smaller there. Indeed the maximum value of k in this case is -0.6, while in the 5-inch channel it is -0.5.

As a matter of interest it could be mentioned that if the basis of comparison is not Reynolds number but maximum mean speed (for the 1-inch channel U_o = 15 m/sec) then figure 5 shows a distribution of $\tilde{u}'$, $\tilde{v}'$, and $\tilde{w}'$ very similar to that of figure 18, the absolute values being somewhat lower in the 5-inch channel.

RESULTS AND DISCUSSION

Mean-Velocity Distribution

A careful study of the two-dimensional nature of the channel flow was first made. Mean-velocity measurements were carried out at approximately x = -2 inches at different heights in the channel: At positions 6 inches from the bottom, 6 inches from the top, and at the middle. Agreement among the three sets of measurements confirmed the two-dimensionality. A further check was made on possible end effects that might influence the results. The length of the channel was extended by 6 inches and the mean-velocity measurements were repeated at x = -8 inches. No change in the profile was noticed. Figure 6 shows the mean-velocity distributions at three Reynolds numbers, R = 61,600, R = 30,800, and R = 12,300. The distributions follow Von Kármán's logarithmic law very well, except, of course, near the wall and at the center of the channel (fig. 7). The values of U_τ were obtained from the velocity gradients at the wall.

Measurements were made with special care close to the wall. Velocities at a large number of points were recorded within the laminar sublayer in order to establish with reasonable accuracy the shape of the velocity profile at the wall (fig. 8). The thickness of the laminar sublayer (the point where the velocity distribution deviates from the logarithmic law) was found to be $\delta \approx 30 \frac{\nu}{U_\tau}$ (fig. 7).

In figure 8 it can be seen that for the case of the lowest Reynolds number a few points near the wall indicate very low velocities. Since the point at which $\frac{y}{d} = 0$ has been determined with great accuracy and since the equations of motion of the channel flow require a negative curvature for the velocity profile, it was concluded that the hot-wire indicated too low velocities near the wall for the lowest Reynolds number. (The dashed curve for this case in fig. 8 shows the interpolated

velocity distribution for $0 < \frac{y}{d} < 0.01$.) It can be shown that very high local-velocity fluctuations cause the hot-wire to read velocities lower than the true mean value. Since the mean current of the wire varies with the fourth root of the velocity,

$$\sqrt[4]{u} = \sqrt[4]{\bar{u}}\left[\overline{\left(1 + \frac{u'}{\bar{u}}\right)^2 + \left(\frac{v'}{\bar{u}}\right)^2 + \left(\frac{w'}{\bar{u}}\right)^2}\right]^{1/8}$$

where u is the velocity to which the hot-wire responds and $\bar{u}$ is the true mean velocity. Near the wall $\overline{\left(\frac{v'}{u}\right)^2} \ll 1$ and can therefore be neglected. Because of the cosine-type directional characteristics of the hot-wire the effect of the w'-fluctuation can also be neglected. The velocity measured by the wire can be written, after expanding the above expression, as

$$u = \bar{u}\left[1 - \frac{3}{16}\overline{\left(\frac{u'}{\bar{u}}\right)^2} + \cdots\right]$$

Since the average of the odd terms is zero the series converges rapidly. In the region in question, the velocity fluctuations obtained were very high indeed $\left(\frac{\tilde{u}'}{u} > 0.30\right)$. Their absolute values, however, are probably even larger, since the nonlinearity effect of the large fluctuations on the hot-wire response still further amplified by the very low mean velocities is not taken into account because the wire-length corrections are neglected. The mean-velocity correction therefore given by the above relation is too small to give the required negative curvature of the profile.

Turbulence Levels

Figures 9 to 14 represent the results of measurements of the three components $\tilde{u}'$, $\tilde{v}'$, and $\tilde{w}'$ of the turbulent-velocity-fluctuation distribution in the channel for the three Reynolds numbers.

The velocity fluctuations $\tilde{u}'$ relative to local speeds increase very rapidly near the wall as is shown in figures 9 and 10. Measurements very close to the wall indicate that $\tilde{u}'/u$ reaches a maximum within the laminar boundary layer $\left(yU_\tau/\nu \approx 17\right)$ and it tends toward a constant value at the wall which is independent of the Reynolds number. This point will be discussed in detail under Reynolds Number Effect.

The absolute values of the distribution of $\tilde{u}'$ show the same general shape as that obtained by Reichardt (reference 9), having the characteristic maximum near the wall and thus showing the strong action of viscosity even for values of $y \approx 48$.

Using the x-type hot-wire technique for obtaining the velocity-fluctuation components v' and w', no measurements could be obtained near the wall. Figures 13 and 14 show that, while in the center of the channel the magnitudes of $\tilde{v}'$ and $\tilde{w}'$ are the same, $\tilde{w}'$ increases faster toward the wall. This agrees with the ultramicroscope measurements in a pipe by Fage and Townend (reference 18).

No length corrections were necessary to the measurements of u' except near the wall; however, no corrections were applied in this region since no measurements of λ_z could be made. In this region, furthermore, the fluctuations are very large and the values given in figure 10 must be accepted with reserve. The hot-wire response for large velocity fluctuations is not well understood yet and no correction was attempted. Length corrections were applied to the measurements of v' and w'.

Correlation Coefficient and Shear Distribution

The correlation coefficient is fairly constant across most of the channel (fig. 15) as indicated already by Wattendorf and Kuethe (reference 6). The maximum values of k obtained decrease slowly with increasing Reynolds number and thus show a definite Reynolds number dependence. Existing results indicate, however, that parameters other than Reynolds numbers also influence the value of k. The following table shows magnitudes of the maximum correlation coefficient as obtained by different investigators working with channels of various widths and with various Reynolds numbers:

Experiments by	Channel width (cm)	R	k_{max}
Reichardt (reference 9)	24.6	8,000	−0.45
Laufer (present paper)	2.5 (1 in.)	12,200	−.63
Laufer (present paper)	12.7 (5 in.)	12,300	−.50
Wattendorf (reference 7)	5.0	15,500	−.52
Laufer (present paper)	12.7 (5 in.)	30,800	−.45
Laufer (present paper)	12.7 (5 in.)	61,600	−.40

Wattendorf obtained his value of k from his measurements of the quantities $\tilde{u}'/U_o$, $\tilde{v}'/U_o$, and $\overline{u'v'}/U_o^2$. Unfortunately his preliminary

measurements of $\tilde{v}'$ are incorrect; their magnitude is larger than that of $\tilde{u}'$ at all values of y across the channel contrary to results obtained by Reichardt and by the present writer. Wattendorf himself points out the inaccuracy of the values of $\tilde{v}'$ in his paper. Because of the large values of v' his computed correlation coefficients are too low. The value $k_{max} = -0.52$ listed in the above table was obtained by using Wattendorf's values $\frac{\overline{u'v'}}{U_o^2} = 0.001$ and $\frac{\tilde{u}'}{U_o} = 0.055$ and the value $\frac{\tilde{v}'}{U_o} = 0.035$ $\left(\frac{y}{d} = 0.5\right)$ obtained by the author for both the 1-inch (2.5-cm) and 5-inch (12.7-cm) channel at $R = 12{,}200$ and $R = 12{,}300$, respectively.

The variation of k indicates that for the same Reynolds number the correlation coefficient tends to increase with increasing maximum mean velocity (i.e., in a channel of decreasing width).

Figures 16 to 18 show the distribution of all the measured quantities including the shear distribution. For the case of the two higher Reynolds numbers, three independent measurements were made for the determination of the shear distribution by methods indicated in Equations of Motion for Two-Dimensional Channel Flow. Figure 19 indicates that consistent results are obtained for the value of τ whether calculated from the pressure gradient along the channel or from the velocity gradient at the wall. The turbulent-shear distributions obtained from hot-wire measurements and those calculated from figure 17 show satisfactory agreement. However, for the flow at the highest Reynolds number, the hot-wire measurements gave a 20-percent-lower value for the shear coefficient, as may be seen in figure 18.[4] At present, the writer can give no satisfactory explanation for this discrepancy. In the flow at the lowest Reynolds number, no pressure measurements were made because the very low pressure gradient (approx. 0.0003 mm of alcohol/cm) did not permit accurate measurements. However, in this case the wall shear computed from the measured mean fluctuating quantities $\tilde{u}'$, $\tilde{v}'$, and k and the mean-velocity measurements may be compared with that obtained in the 1-inch-channel flow having nearly the same Reynolds number. The comparison shows satisfactory agreement: For the 1-inch channel $\frac{\tau_o}{\rho U_o^2} = 0.0019$; for the 5-inch channel $\frac{\tau_o}{\rho U_o^2} = 0.0018$.

---

[4]This result was accepted after the absolute values were carefully checked; the v'-wire response was compared with u'-fluctuations in an isotropic field and the two-dimensional character of the flow was checked.

Scale and Microscale Measurements

For a further understanding of the structure of the turbulent field, correlations of u'-fluctuations at two different points were carried out. Since the field is not isotropic, the scale and microscale measurements were repeated both in the y- and z-direction for different values of y/d.

R_z-correlations.- Figure 20 shows typical R_z-correlation distributions at different values of y/d corresponding to $R = 30,800$. For larger values of z, inaccuracies in the measurements did not permit the exploration of the negative region of the correlation distribution. From the measured distributions of R_z at four stations across the channel and for different values of R, the values of L_z and λ_z were calculated (figs. 21 and 22). In these figures L_z is seen to be decreasing uniformly toward the wall, while λ_z reaches a definite maximum at about $\frac{y}{d} = 0.7$ and then decreases with decreasing y/d.

R_y-correlations.- Distributions of the R_y-correlation at a given value of y/d were obtained by fixing the stationary hot-wire at the given value of y/d and traversing with the moving hot-wire away from the fixed one toward the channel center. Values of L_y and λ_y were then calculated from these distributions of R_y. In the region $1.0 > \frac{y}{d} > 0.1$ the gradients of the various quantities are slight; no significant asymmetry in the function R_y is therefore expected. Measurements of the top part of the R_y-correlation distribution $(1.0 > R_y > 0.8)$ by Prandtl and Reichardt (reference 19) justify this belief fairly well.

By comparing figure 20 with figure 23, the strong effect of the existing nonisotropy can immediately be seen. Although both R_y and R_z correspond to Von Kármán's g-function (reference 10) they exhibit different behaviors across the channel. The R_z-correlation function falls more and more rapidly to zero with decreasing y/d. Traversing from $\frac{y}{d} = 1.0$ to $\frac{y}{d} = 0.70$ the distribution of R_y is found to behave similarly; however, the dashed curve measured at $\frac{y}{d} = 0.4$ (fig. 23) indicates considerably increased correlations for larger values of Y. It is thus seen that around $\frac{y}{d} = 0.7$ there is a definite decrease in energy content of the fluctuations having low frequencies. Further consideration of this fact is given later in the discussion of the energy balance in the channel.

The values of $L_y = \int_0^\infty R_y \, dY$ (fig. 21) are not so reliable as those of L_z since R_y could not be measured at sufficiently large values of Y because of the limitation of the traversing mechanism used.

The distribution of λ_y across the channel is similar to that of λ_z (fig. 22). From $\frac{y}{d} = 1.0$ to $\frac{y}{d} \approx 0.7$ both λ_y and λ_z increase almost proportionally to u', indicating that the turbulent-energy dissipation $W \sim \frac{\overline{u'^2}}{\lambda^2}$ is approximately constant in this region. It should be noticed, however, that λ_z is consistently larger than λ_y throughout the channel cross section. Some measurements of λ_y close to the wall are also indicated in figure 23. No length correction was found to be necessary for the measured values of λ_y and λ_z.

A rough estimate of L_x by the method already described gave a value approximately twice that of L_z at the center of the channel (fig. 21). Its value increases to a maximum at $\frac{y}{d} \approx 0.5$ and then decreases rapidly. No values for L_x are given for the lowest Reynolds number; in this case the value of σ is very close to unity and, since L_x is proportional to $\frac{1}{\sigma - 1}$, σ should be known within an accuracy of 1 percent to give consistent results for L_x. Unfortunately measurements of L_x cannot be made with this accuracy, particularly when the u'-fluctuations are of rather low frequencies as is the case for $R = 12{,}300$. It should be mentioned that the accuracy of the determination of L_x is more limited by the inaccurately measured value of σ than by the fact that an approximate spectrum function $F(n)$ is used in equation (9).

The distribution of λ_x obtained by the differentiation method shows the same behavior as that of λ_y and λ_z (fig. 22). It has the characteristic maximum at $\frac{y}{d} \approx 0.7$. No measurements were made for $R = 12{,}300$ because of the inaccuracy due to the large noise-to-signal ratios.

As a matter of interest the results of some measurements of λ_x obtained with the zero-counting method are compared with those described above. (See fig. 22.) Since the validity of the assumptions involved in this method is not clarified yet, these measurements should be regarded as preliminary.

Spectrum Measurements

The spectrums of the velocity fluctuations $\overline{u'^2}$ have been obtained at various values of y/d across the channel. With improved instrumentation it was possible to reduce experimental scatter by a considerable amount. The accuracy of the present measurements is believed to be within ±10 percent with the exception of values corresponding to low frequencies ($n < 100$ cps) because of the large-amplitude fluctuations and with the exception of values corresponding to high frequencies ($n > 4000$ cps) because of noise and of possible wire-length effect. A typical spectrum distribution taken at $\frac{y}{d} = 1.00$ is shown in figure 24. (The measured spectrums at various positions of y/d are given in table I.) No attempt is made to compare the measured distributions with existing theories since the restrictive assumptions of these theories (isotropy and flows at high Reynolds numbers) are not satisfied in the present experiments. The only frequency range where comparison is possibly justified is the viscous region, that is, the high-frequency part of the spectrum where viscosity plays a dominant role. Unfortunately here the accuracy of the measurements is not good enough to afford any definite conclusions. Therefore, the rather close agreement of the measured spectrum (for all values of y/d except in the laminar sublayer) with the n^{-7}-law predicted by Heisenberg (reference 2) should be accepted with reserve (fig. 24).

For a comparison of the energy spectrums at different points in the channel, figure 25 shows the distribution of $n^2F(n)$ instead of that of $F(n)$ as a function of the frequency. This method of presentation emphasizes energies corresponding to the higher frequencies but gives a clearer over-all comparison of the different sets of measurements. The characteristic maximum of the distribution of λ_x immediately becomes apparent in this figure. From the fact that the correlation coefficient is a Fourier transform of the spectrum function it follows that

$$\left(\frac{\partial^2 R_x}{\partial x^2}\right)_{x=0} = \frac{1}{\lambda_x} = \frac{4\pi^2}{u^2}\int_0^\infty n^2 F(n)\, dn$$

Thus λ_x can be computed from the distributions of $n^2F(n)$. The calculated values check within a few percent with direct measurements (fig. 22).

Reynolds Number Effect

Figure 7 shows the distribution of mean velocities plotted in the form of "friction velocity" u/U_τ against "friction-distance parameter" yU_τ/ν. In this form the profiles are independent of the Reynolds number $U_o d/\nu$ and follow Von Kármán's logarithmic law:

$$\frac{u}{U_\tau} = A \log \frac{yU_\tau}{\nu} + B$$

The constants A and B are 6.9 and 5.5, respectively. Comparing the present measurements with previous ones it is to be noted that because of the very smooth wall surfaces used, the value B is larger than that of other investigators. Making allowances for this effect, measurements are in fairly good agreement with those of Doench (reference 4) and Reichardt (reference 9). Nikuradse's channel results (reference 5) differ from all other existing experiments. It is pertinent to mention that for the Reynolds number range in question ($R < 100{,}000$) the slope of the logarithmic mean-velocity distribution (the constant A) both in pipes and channels is larger than that established by Nikuradse's pipe measurements ($A = 5.75$).

The Reynolds number has a definite influence on the velocity fluctuations also. Along most of the cross section where the influence of the viscosity is negligible the fluctuations $\tilde{u}'$, $\tilde{v}'$, and $\tilde{w}'$ decrease slowly with increasing Reynolds number.

Very close to the wall, according to Prandtl's hypothesis, all velocities of the form Velocity/U_τ must be a function of the friction-distance parameter only. It has already been pointed out that the mean velocity obeys this similarity law. Figure 26 shows the distribution of $\tilde{u}'/U_\tau$ as a function of yU_τ/ν for the different flow conditions investigated. The following remarks can be made with reference to this figure:

(1) For values of $\frac{yU_\tau}{\nu} < 100$, values of $\tilde{u}'/U_\tau$ corresponding to the various cases indicate similar behavior. They reach a maximum at about $\frac{yU_\tau}{\nu} \approx 17$.

(2) It is believed that the similarity is actually more complete than indicated in figure 26. Because the microscale is not known in regions very close to the wall no length corrections could be applied. These corrections would of course be appreciably higher for the two high-velocity flows ($R = 61{,}600$, $2d = 5$ in. and $R = 12{,}200$, $2d = 1$ in.), and would therefore bring the various distributions of $\tilde{u}'/U_T$ closer together in the region in question.

(3) The effect of viscosity is more pronounced on the fluctuating quantities than on the mean velocity.

(4) Taylor pointed out in 1932 (supporting his arguments by Fage and Townend's ultramicroscope measurements) that $\tilde{u}'/u$ and $\tilde{w}'/u$ approach a finite value at the wall (reference 18). It follows from the similarity law that this value should be an absolute constant independent of the Reynolds number. Figure 10 indicates this to be true, the constant being $(\tilde{u}'/u)_{y=0} \approx 0.18$.

It is of considerable interest to discuss the variation of the scale and microscale with Reynolds number. For flows behind grids where the turbulence is isotropic the scale is independent of the mean velocity and depends on the mesh size of the grid. Similar behavior was found for the channel flow. Figure 21 shows the distributions of L_y and L_z for different velocities. These distributions indicate no consistent variation with velocity. Furthermore, measurements in a 1-inch channel give a value for L_z five times lower and a ratio for L_y somewhat larger than the values obtained in the present investigation.

The variation of λ depends, of course, on the velocity and channel width. The values of λ decrease with increasing velocity; however, the variation of λ with channel width is less than that of L.

Fully Developed Character of Turbulence

The flow in the channel is called fully developed if the variations of the mean values of the velocity and the mean squares of the velocity fluctuations with x are very small. That the mean velocity profile does not vary downstream is evident from the pressure-gradient measurements (fig. 19). The gradient in x of $\overline{u'^2}$ was measured on the axis of the channel. It was found that $\overline{u'^2}$ was indeed decreasing with x. The gradient, however, was very small as compared with $\frac{1}{\rho}\frac{\partial p}{\partial x}$:

$$\frac{\partial \overline{u'^2}}{\partial x} \approx 0.01 \frac{1}{\rho}\frac{\partial p}{\partial x}$$

Hence for all practical purposes $\partial\overline{u'^2}/\partial x$ can be neglected. No measurements have been made concerning $\partial\overline{u'v'}/\partial x$, since the scatter in the values would cover any effect. However, there is little doubt that $\partial\overline{u'v'}/\partial x$ is of the same order as $\partial\overline{u'^2}/\partial x$ and that the use of equations (3a) and (3b) is therefore justified here.

Energy Balance in Fluctuating Field

The energy equation for a two-dimensional channel has the form given by equation (8) and is valid throughout the cross section of the channel with the exception of a small region near the wall. The term $\tau\frac{du}{dy}$ on the left side of equation (8) corresponds to the energy produced by the shearing stresses and it can be obtained directly from the measurements of τ and from the mean velocity profile. The second term on the right $\mu\overline{\left(\frac{\partial u_i'}{\partial x_j}\right)\left(\frac{\partial u_i'}{\partial x_j}\right)}$ expresses the amount of energy that is being dissipated because of the breaking down of the larger eddies to smaller ones. The term may be written explicitly

$$W = \mu\left[2\overline{\left(\frac{\partial u'}{\partial x}\right)^2} + 2\overline{\left(\frac{\partial v'}{\partial y}\right)^2} + 2\overline{\left(\frac{\partial w'}{\partial z}\right)^2} + \overline{\left(\frac{\partial v'}{\partial x} + \frac{\partial u'}{\partial y}\right)^2} + \overline{\left(\frac{\partial w'}{\partial y} + \frac{\partial v'}{\partial z}\right)^2} + \overline{\left(\frac{\partial u'}{\partial z} + \frac{\partial w'}{\partial x}\right)^2}\right]$$

The problem is to express these functions in terms of easily measurable quantities. In the case of isotropic turbulence Taylor solved the problem by introducing the microscale of turbulence λ, and obtained for the dissipation

$$W = 15\mu\frac{\overline{u'^2}}{\lambda^2} \qquad (10)$$

It is attempted here to carry over his analysis to the case of channel flow. The following assumptions have to be made in this connection:

(a) The gradient of the velocity fluctuations is small in all three directions. With the exception of the region near the wall this is justifiable from the measurements.

(b) Since only correlations of u' have been measured, it is assumed that the correlations of w' as functions of Z (Von Kármán's f-function) have the same curvature at the origin ($Y = Z = 0$) as the correlation of u' has as a function of X; that is,

$$\left(\frac{\partial^2 R_Z w'}{\partial Z^2}\right)_0 = \left(\frac{\partial^2 R_X u'}{\partial X^2}\right)_0 = -\frac{1}{\lambda_X^2}$$

Furthermore the correlations of v' as functions of X and Z and the correlations of w' as functions of X (Von Kármán's g-functions) have the same curvature at the origin as the correlation of u' has as a function Z; that is,

$$\left(\frac{\partial^2 R_X v'}{\partial X^2}\right)_0 = \left(\frac{\partial^2 R_Z v'}{\partial Z^2}\right)_0 = \left(\frac{\partial^2 R_X w'}{\partial X^2}\right)_0 = \left(\frac{\partial^2 R_Z u'}{\partial Z^2}\right)_0 = -\frac{2}{\lambda_Z^2}$$

Finally,

$$\left(\frac{\partial^2 R_Y v'}{\partial Y^2}\right)_0 = \left(\frac{\partial^2 R_Y w'}{\partial Y^2}\right)_0 = \left(\frac{\partial^2 R_Y u'}{\partial Y^2}\right)_0 = -\frac{2}{\lambda_Y^2}$$

(c) The cross products were calculated using similar arguments; thus,

$$\overline{\frac{\partial v'}{\partial x}\frac{\partial u'}{\partial y}} = -\frac{1}{2}\frac{\tilde{v}'}{\lambda_Z}\frac{\tilde{u}'}{\lambda_Y}$$

$$\overline{\frac{\partial w'}{\partial y}\frac{\partial v'}{\partial z}} = -\frac{1}{2}\frac{\tilde{w}'}{\lambda_Y}\frac{\tilde{v}'}{\lambda_Z}$$

$$\overline{\frac{\partial u'}{\partial z}\frac{\partial w'}{\partial x}} = -\frac{1}{2}\frac{\tilde{u}'}{\lambda_Z}\frac{\tilde{w}'}{\lambda_Z}$$

With these assumptions the derivatives of the fluctuations could be expressed in terms of the measured values of λ_x, λ_y, and λ_z:

$$W = \mu\left[\frac{2}{\lambda_x^2}\left(\overline{u'^2} + \overline{w'^2}\right) + \frac{2\overline{v'^2}}{\lambda_y^2} + 2\frac{\overline{v'^2}}{\lambda_z^2} - \frac{\tilde{u}'\tilde{v}'}{\lambda_z\lambda_y} + 2\frac{\overline{u'^2}}{\lambda_y^2} + 2\frac{\overline{w'^2}}{\lambda_y^2} - \frac{\tilde{v}'\tilde{w}'}{\lambda_y\lambda_z} + 2\frac{\overline{v'^2}}{\lambda_z^2} + 2\frac{\overline{u'^2}}{\lambda_z^2} - \frac{\tilde{u}'\tilde{w}'}{\lambda_z^2} + 2\frac{\overline{w'^2}}{\lambda_z^2}\right]$$

At the middle of the channel W turned out to be 2.86 ergs per cubic centimeter per second for R = 30,800. Using the isotropic relation

$$W = 15\mu\frac{\overline{u'^2}}{\lambda_y^2} = 15\mu\frac{\overline{u'^2}}{\lambda_x^2} = 15\mu\frac{\overline{u'^2}}{\lambda_z^2}$$

the values 2.88, 4.38, and 2.24 ergs per cubic centimeter per second were obtained depending upon whether λ_x, λ_y, or λ_z was used. (For the value of $\overline{u'^2}$ the algebraic mean of the squares of the fluctuations was used.)

Figure 27 shows the distribution of W in the center region of the channel. Taylor obtained a similar distribution of the dissipated energy across the channel (reference 20); however, his numerical magnitudes are too high since he substituted in the isotropic relation, in equation (10), the values of λ_y, which turn out to be less than those of λ_x and λ_z.

From the known distributions of the energy production and dissipation the diffusion of energy is easily calculated from equation (8). It should be pointed out that because of the approximations involved in the calculation of the dissipation and diffusion terms, the conclusions derived from them are more or less of a qualitative nature. It is seen from figure 27 that at $\frac{y}{d} \approx 0.7$ the diffusion term is zero. It was also pointed out earlier that in this region the R_y-correlations show a considerable change in shape indicating a shift in energy from the lower to higher frequencies of the velocity fluctuations. These two facts suggest that the energy diffusion is associated mainly with the low frequencies of the fluctuations.

The equation expressing the balance of the three forms of energy furnishes the following picture of the turbulent flow field in the channel where viscous dissipation is still negligible: Two planes passing through points where the diffusion of energy vanishes divide the channel flow into three parts. From these planes energy is being transported toward the channel center and the walls. The middle region, the width of which is of the order of L_x, receives most of its energy by diffusive action and this energy is dissipated here at a constant rate. In the two outside regions all three energy terms increase rapidly, the production term being the dominant one, and their interaction is more involved.

This picture of the flow field is only of a descriptive nature. The purpose of further investigations should be to obtain information on the development and mechanism of such an energy balance.

Locally Isotropic Character of Turbulent Channel Flow

The concept of locally isotropic turbulence obtained by Kolmogoroff requires the smaller eddies in turbulent flow to approach isotropy. Smaller eddies are the ones with length dimension l small compared with the scale of turbulence L. The smallest characteristic length in turbulent motion is Kolmogoroff's η defined as

$$\eta = \left(\frac{\nu^3}{\epsilon}\right)^{1/4}$$

where ϵ is the total dissipated energy. Clearly, to approach locally isotropic conditions it is necessary that

$$L \gg \eta$$

It follows from this hypothesis that beyond sufficiently high frequencies (of the order of $\tilde{u}'/\eta$, say) no correlations exist between the components of the velocity fluctuations. Figure 28 shows the measured spectrum of $\overline{u'^2}$ as compared with the spectrum of $\overline{u'v'}$ at $\frac{y}{d} = 0.4$. It is seen that the shear spectrum tends to zero at a frequency of about 1500 cycles per second while $F_{\overline{u'^2}}(n)$ still has a detectable value at 5000 cycles per second. This result verifies Kolmogoroff's assumption. It should be mentioned that the absolute values of $F_{\overline{u'v'}}(n)$ are not so accurate as those of $F_{\overline{u'^2}}(n)$ since they represent the small difference between two large values of hot-wire signal.

It is to be noted that even though local isotropy was shown to exist in the channel flow, the values of the various vorticity terms $\left(\frac{\overline{u_i^2}}{\lambda_j^2}\right)$ differ appreciably, indicating that the relative magnitudes of these terms do not constitute a sensitive test for the existence of local isotropy. This is evident from the comparison of the distributions $n^2F_{\overline{u'^2}}(n)$ and $n^2F_{\overline{u'v'}}(n)$ (fig. 28). It is apparent from the figures that a large part of the contribution to $\int_0^\infty n^2F(n)\,dn$ comes from a frequency well below 1500 cycles per second. Local isotropy, according to the shear spectrum, exists only above a frequency of 1500 cycles per second.

CONCLUDING REMARKS

The measurements presented here confirm the general conceptions concerning the mean velocity profile in a turbulent channel. The extent of the laminar sublayer, the velocity profile in the sublayer, and the over-all velocity distribution as measured here are in good agreement with general theoretical expectations.

Measurements of the turbulent field show that the hot-wire technique is well enough developed to give consistent results for the intensities and correlation functions.

Detailed measurements of the velocity fluctuations in the direction of the flow u' were carried out well within the laminar sublayer. It was found that the similarity law for $\tilde{u}'/U_\tau$, where U_τ is friction velocity, holds fairly well in the vicinity of the wall and as a consequence the magnitude of $\tilde{u}'/u$, where u is local mean velocity, approaches an absolute constant at the wall (approx. 0.18), the value being independent of the Reynolds number. The magnitudes of the velocity fluctuations normal to the flow in the lateral and vertical directions $\tilde{v}'$ and $\tilde{w}'$ are nearly the same in the middle region of the channel, $\tilde{w}'$ increasing more rapidly toward the wall.

The measured microscales of turbulence λ_x, λ_y, and λ_z consistently show a maximum at $\frac{y}{d} \approx 0.7$, where y is lateral distance and d is half width of the channel; they increase proportionally with $\tilde{u}'$, indicating a constant rate of energy dissipation W in the center portion of the channel since $W \sim \frac{\overline{u'^2}}{\lambda^2}$.

The scales of turbulence L_y and L_z in the center region are independent of Reynolds number and depend only on the channel width. The microscales, however, show a dependency on the Reynolds number.

From the calculated magnitudes of the energy produced by the shearing stresses and of the dissipated energy a descriptive picture of the energy diffusion in the center region of the channel is obtained.

The spectrum measurements of the $\overline{u'^2}$-fluctuations tend to indicate that $F_{\overline{u'^2}}(n)$ behaves as n^{-7} over a large band in the high-frequency region (where $F_{\overline{u'^2}}(n)$ is fraction of turbulent energy associated with band width dn and n is frequency). From the comparison of the spectrums of $\overline{u'^2}$ and of the turbulent shear the existence of local isotropy in the channel flow is verified.

Guggenheim Aeronautical Laboratory
California Institute of Technology
Pasadena, Calif., September 1, 1949

REFERENCES

1. Kolmogoroff, A.: The Local Structure of Turbulence in Incompressible Viscous Fluid for Very Large Reynolds' Numbers. Comp. rend., acad. sci. URSS, vol. 30, no. 4, Feb. 10, 1941, pp. 301–305.

2. Heisenberg, W.: Zur statistichen Theorie der Turbulenz. Zeitschr. Phys., Bd. 124, Heft 7/12, 1948, pp. 628–657.

3. Onsager, Lars: The Distribution of Energy in Turbulence. Abstract, Phys. Rev., vol. 68, nos. 11 and 12, second ser., Dec. 1 and 15, 1945, p. 286.

4. Doench, F.: Divergente und konvergente turbulente Stroemungen mit kleinen Oeffnungswinkeln. Forsch.–Arb. Geb. Ing.–Wes., Heft 282, 1926.

5. Nikuradse, Johann: Untersuchungen über die Strömungen des Wassers in konvergenten und divergenten Kanälen. Forsch.–Arb. Geb. Ing.–Wes., Heft 289, 1929.

6. Wattendorf, F. L., and Kuethe, A. M.: Investigations of Turbulent Flow by Means of the Hot–Wire Anemometer. Physics, vol. 5, no. 6, June 1934, pp. 153–164.

7. Wattendorf, F. L.: Investigations of Velocity Fluctuations in a Turbulent Flow. Jour. Aero. Sci., vol. 3, no. 6, April 1936, pp. 200–202.

8. Reichardt, H.: Die quadratischen Mittelwerte der Längsschwankungen in der turbulenten Kanalströmung. Z.f.a.M.M., Bd. 13, Heft 3, June 1933, pp. 177–180.

9. Reichardt, H.: Messungen turbulenter Schwankungen. Die Naturwissenschaften, Jahrg. 26, Heft 24/25, June 17, 1938, pp. 404–408.

10. Von Kármán, Th.: The Fundamentals of the Statistical Theory of Turbulence. Jour. Aero. Sci., vol. 4, no. 4, Feb. 1937, pp. 131–138.

11. Kovasznay, L.: Calibration and Measurement in Turbulence Research by the Hot–Wire Method. NACA TM 1130, 1947.

12. Liepmann, Hans Wolfgang, and Laufer, John: Investigations of Free Turbulent Mixing. NACA TN 1257, 1947.

13. Townsend, A. A.: Measurement of Double and Triple Correlation Derivatives in Isotropic Turbulence. Proc. Cambridge Phil. Soc., vol. 43, pt. 4, Oct. 1947, pp. 560–570.

14. Liepmann, H. W., Laufer, J., and Liepmann, Kate: On the Spectrum of Isotropic Turbulence. NACA TN to be published.

15. Townsend, A. A.: Measurements in the Turbulent Wake of a Cylinder. Proc. Roy. Soc. (London), ser. A, vol. 190, no. 1023, Sept. 9, 1947, pp. 551–561.

16. Frenkiel, F. N.: Étude statistique de la turbulence theorie de la correlation avec deux fils chauds non compenses. Comp. rend., acad. sci. (Paris), t. 222, 1946, pp. 1377–1378 and 1474–1476.

17. Dryden, Hugh L.: Turbulence Investigations at the National Bureau of Standards. Proc. Fifth Int. Cong. Appl. Mech. (Sept. 1938, Cambridge, Mass.), John Wiley & Sons, Inc., 1939, pp. 362–368.

18. Fage, A., and Townend, H. C. H.: An Examination of Turbulent Flow with an Ultramicroscope. Proc. Roy. Soc. (London), ser. A, vol. 135, no. 828, April 1, 1932, pp. 656–677.

19. Prandtl, L., and Reichardt, H.: Einfluss von Wärmeschichtung auf die Eigenschaften einer turbulenten Strömung. Deutsche Forschung, Heft 21, 1934, pp. 110–121.

20. Taylor, G. I.: Statistical Theory of Turbulence. III – Distribution of Dissipation of Energy in a Pipe over Its Cross-Section. Proc. Roy. Soc. (London), ser. A, vol. 151, no. 873, Sept. 2, 1935, pp. 455–464.

TABLE I.- MEASURED VALUES OF THE SPECTRUM OF $\overline{u'^2}$

Frequency (cps)	F(n) (sec)				
	$\frac{y}{d} = 1.0$	$\frac{y}{d} = 0.7$	$\frac{y}{d} = 0.4$	$\frac{y}{d} = 0.1$	$\frac{y}{d} = 0.005$
30	----------	----------	----------	----------	772×10^{-5} 786
40	561×10^{-5}	585×10^{-5}	571×10^{-5}	664×10^{-5}	618 604
50	----------	----------	----------	----------	519
60	349	464	----------	----------	436
70	----------	----------	----------	----------	373 345
80	273	211	252	308	309
90	----------	----------	----------	----------	254 272
100	186	141	182.5	226	222
125	----------	----------	----------	----------	157 150
150	95.4	77.3	91.6	140	109 114
175	----------	----------	----------	----------	86.5 74.9
200	68.2	52.6	5618	97.2	63.6 63.6
250	23.1	37.9	45.8	64.9	38.6 38.0
300	33.9 34.6	23.5 25.6	32.2 34.7	44.8 51.3	23.8 21.5
400	19.8	15.0	19.17	25.2	8.03
500	18.9	8.09	12.25	15.5	3.74
600	7.57	5.86	7.6	12.5	1.83
700	5.27	4.0	5.14	8.73	1.06
800	3.31	2.67	3.53	6.07	.531
900	2.29	1.77	2.51	4.04	.352
1000	1.50	1.08	1.76	2.99	.185
1200	.764	.677	1.01	1.80	.090
1500	.295	.257	.379	.787	.016
1750	.147	.16	.221	.422	.008
2000	.0832	.0584	.109	.224	.0039
2500	.0192	.0186	.0487	.0873	.00102
3000	.00682	.00668	.0141	.0313	.000354
3500	.00196	.00272	.00492	.00121	.000133
4000	.000855	.00074	.0021	.00435	.0000664
4500	----------	.000608	.00157	.0029	----------
5000	.000170	0	.00052	.00117	----------
5500	----------	----------	----------	.00062	----------
6000	0	----------	.000252	.000313	----------
7000	----------	----------	----------	.000109	----------

NACA

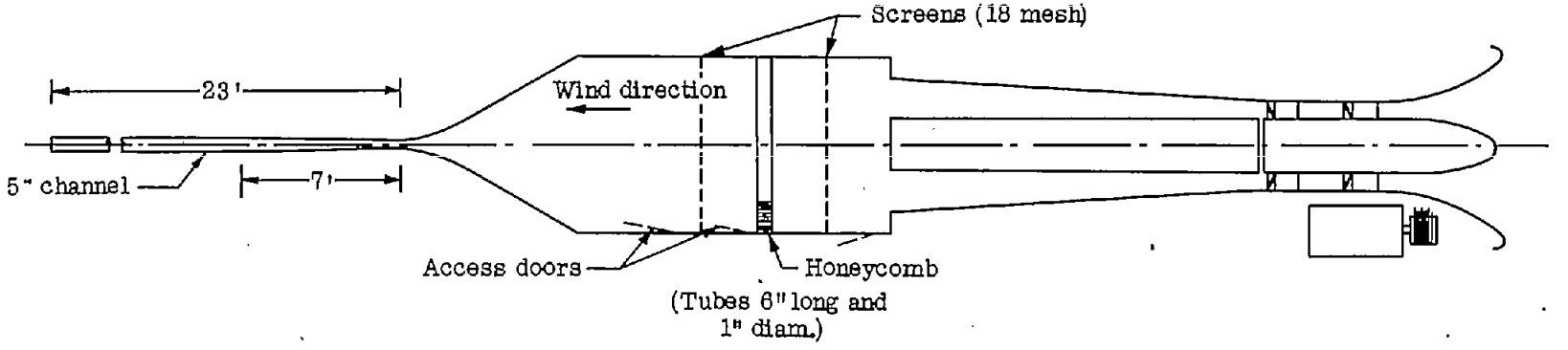

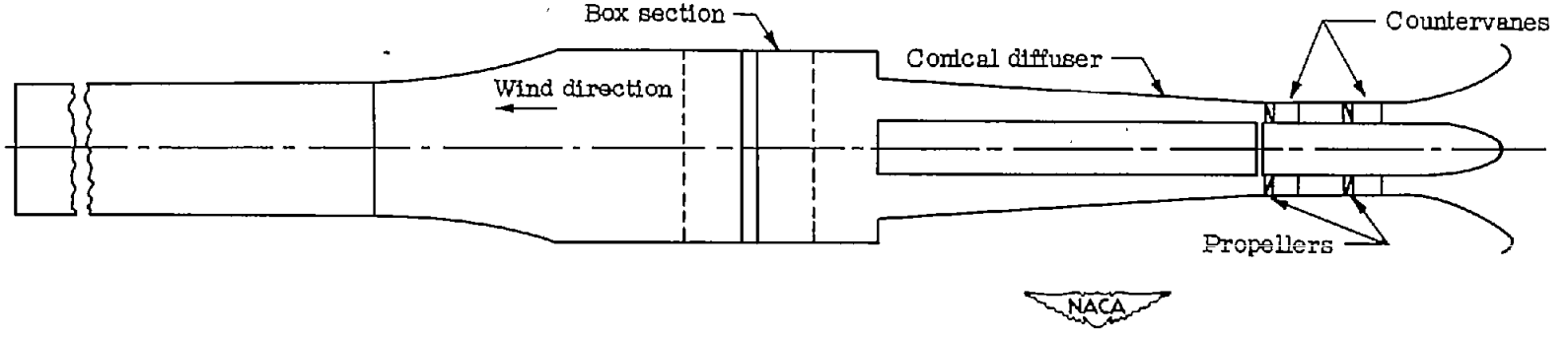

Figure 1.- Diagram of two-dimensional tunnel.

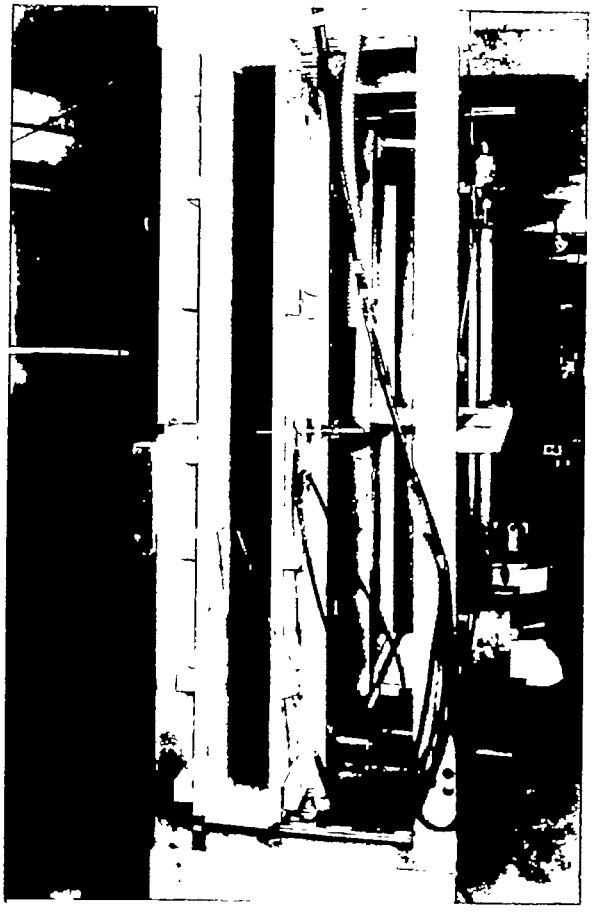

Figure 2.- Exit of channel.

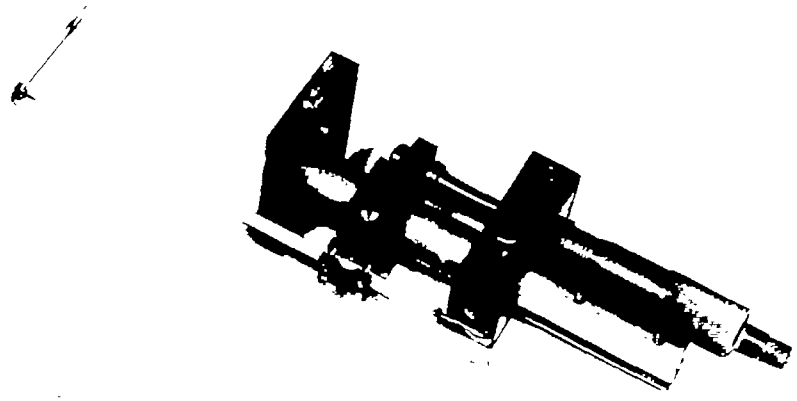

Figure 3.- Traversing mechanism.

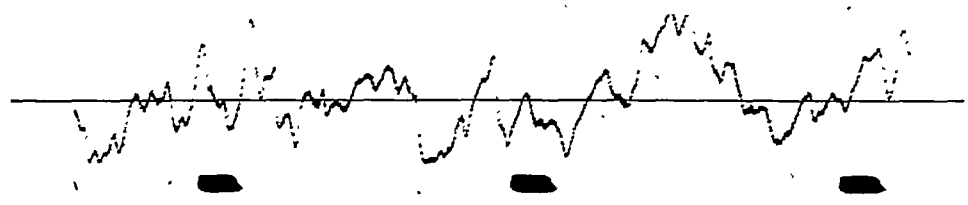

Figure 4.- Typical oscillogram of u'-fluctuation at R = 30,800 and y/d = 1.0. Horizontal line corresponds to u'(t) = 0; interval is approximately 1/20 second.

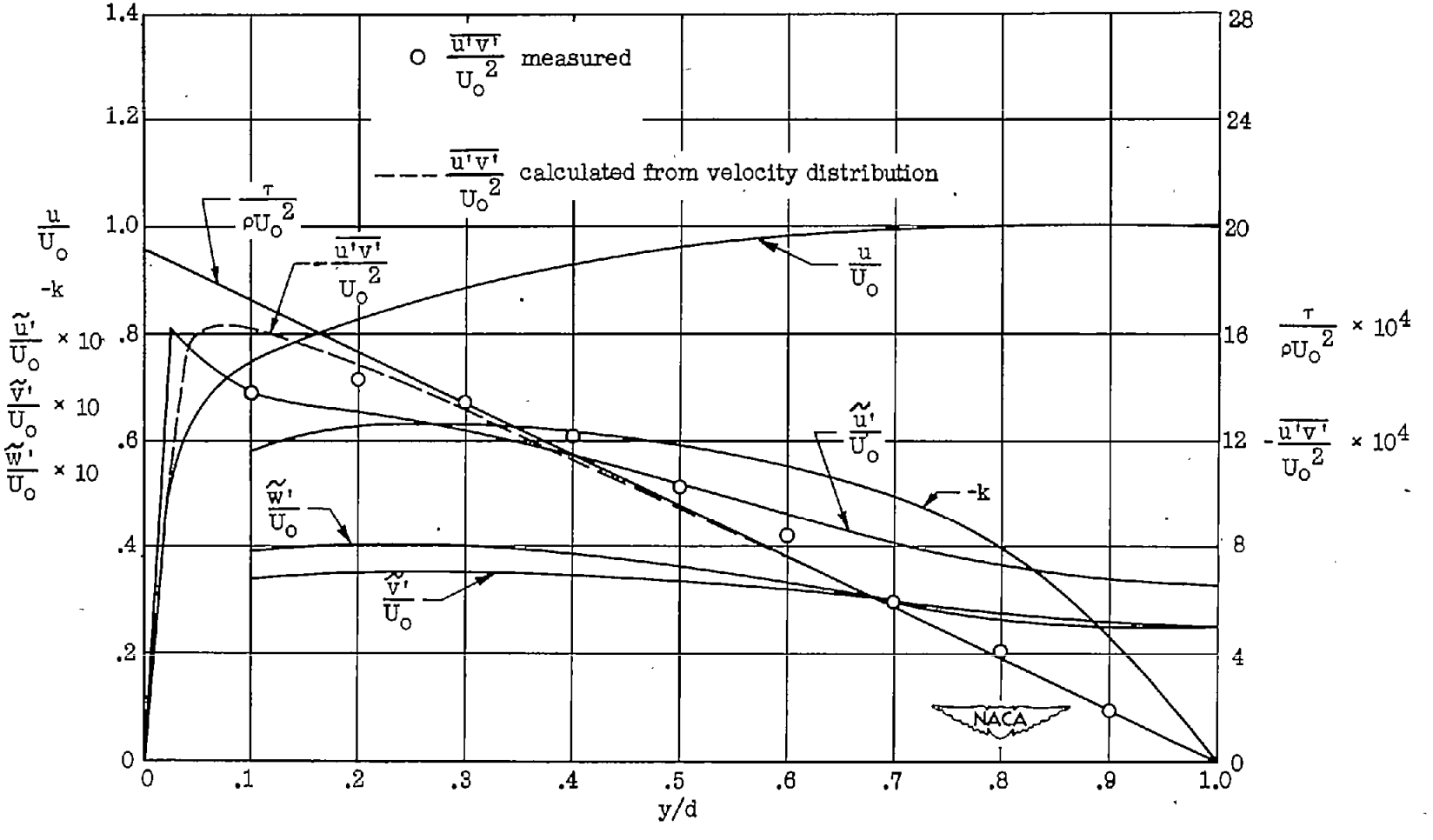

Figure 5.- Distribution of measured quantities across two-dimensional channel of 1-inch width. R = 12,200.

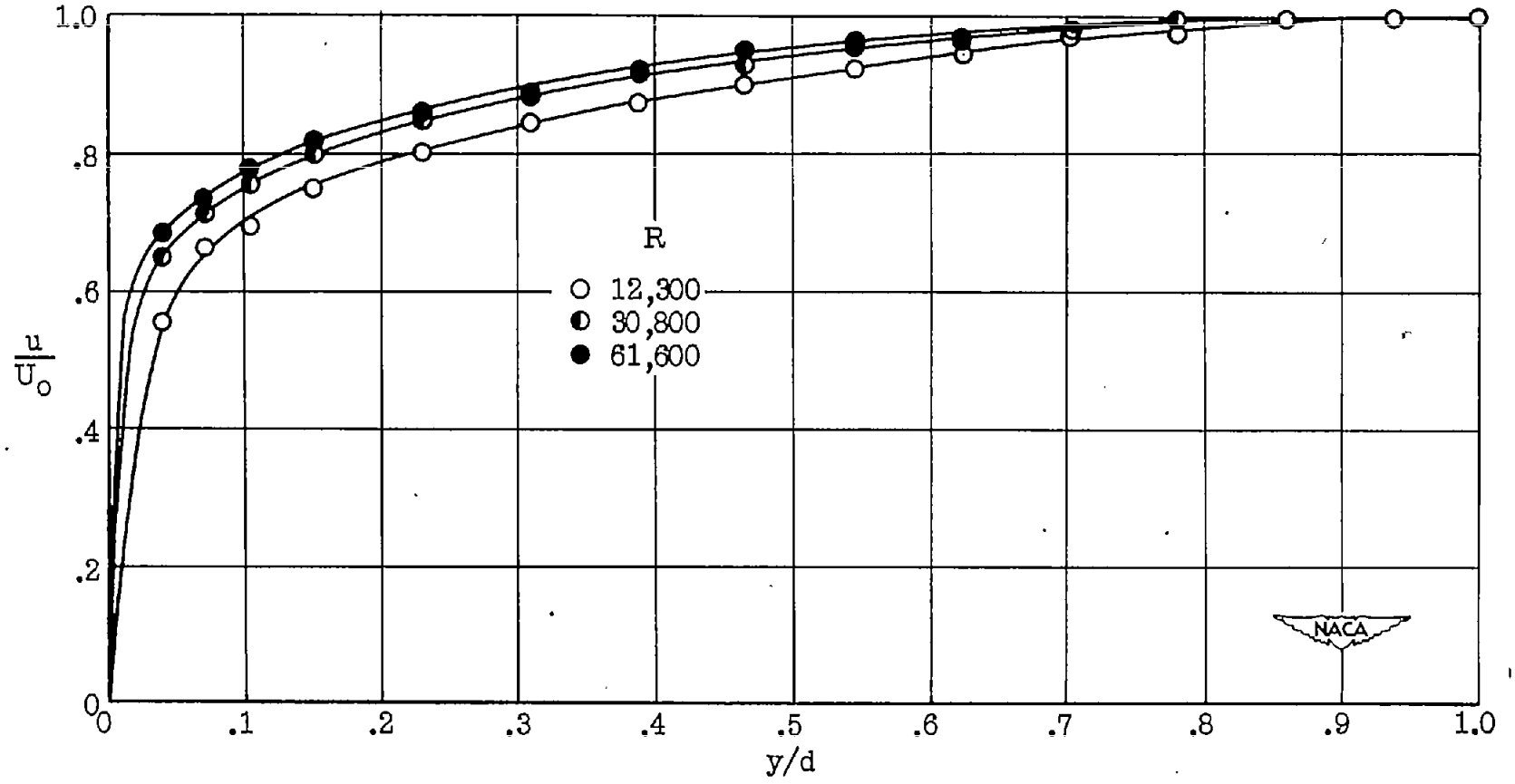

Figure 6.- Mean-velocity distribution. Measured points close to wall are not shown.

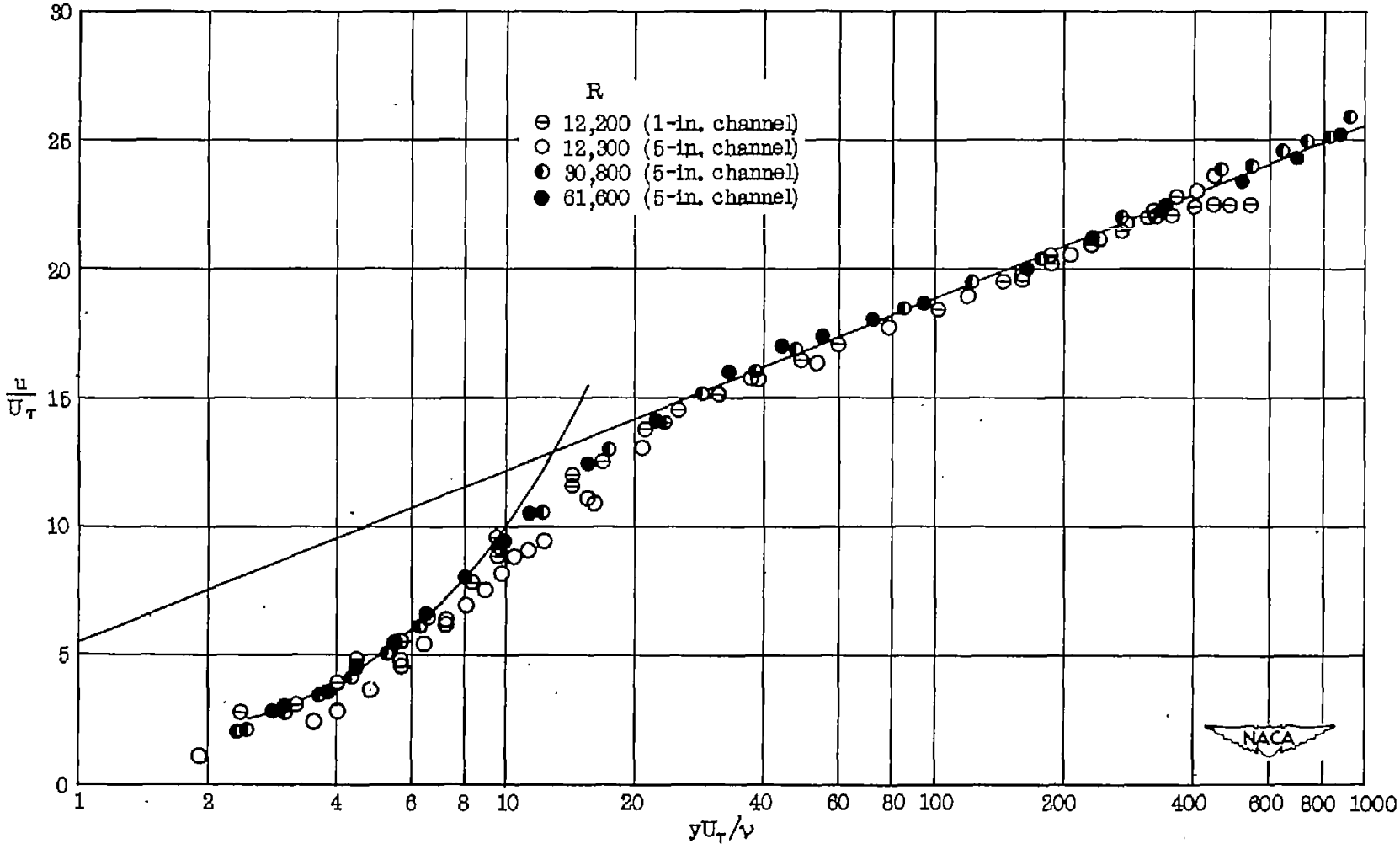

Figure 7.- Logarithmic representation of mean-velocity distribution.

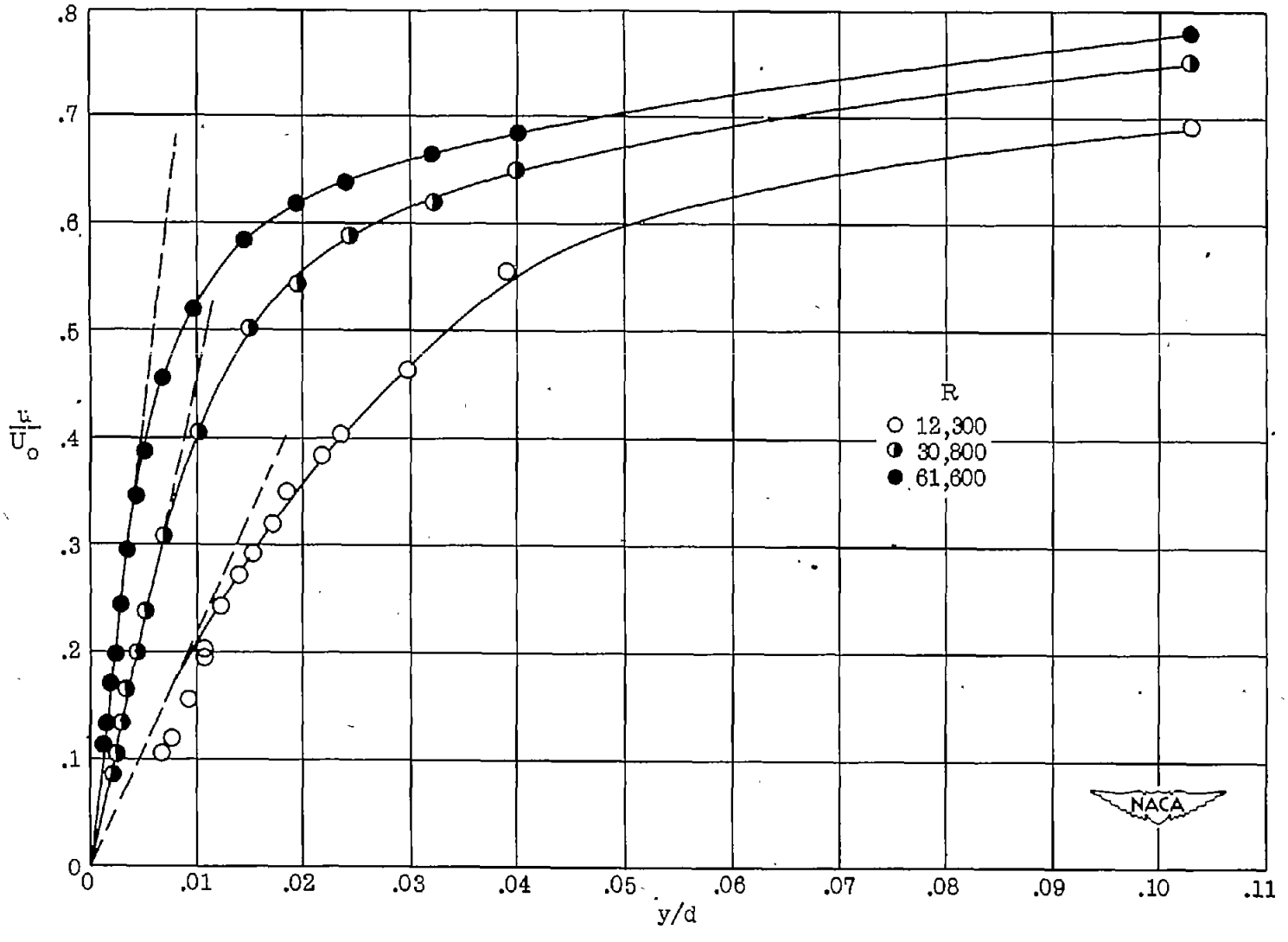

Figure 8.- Mean-velocity distribution near wall.

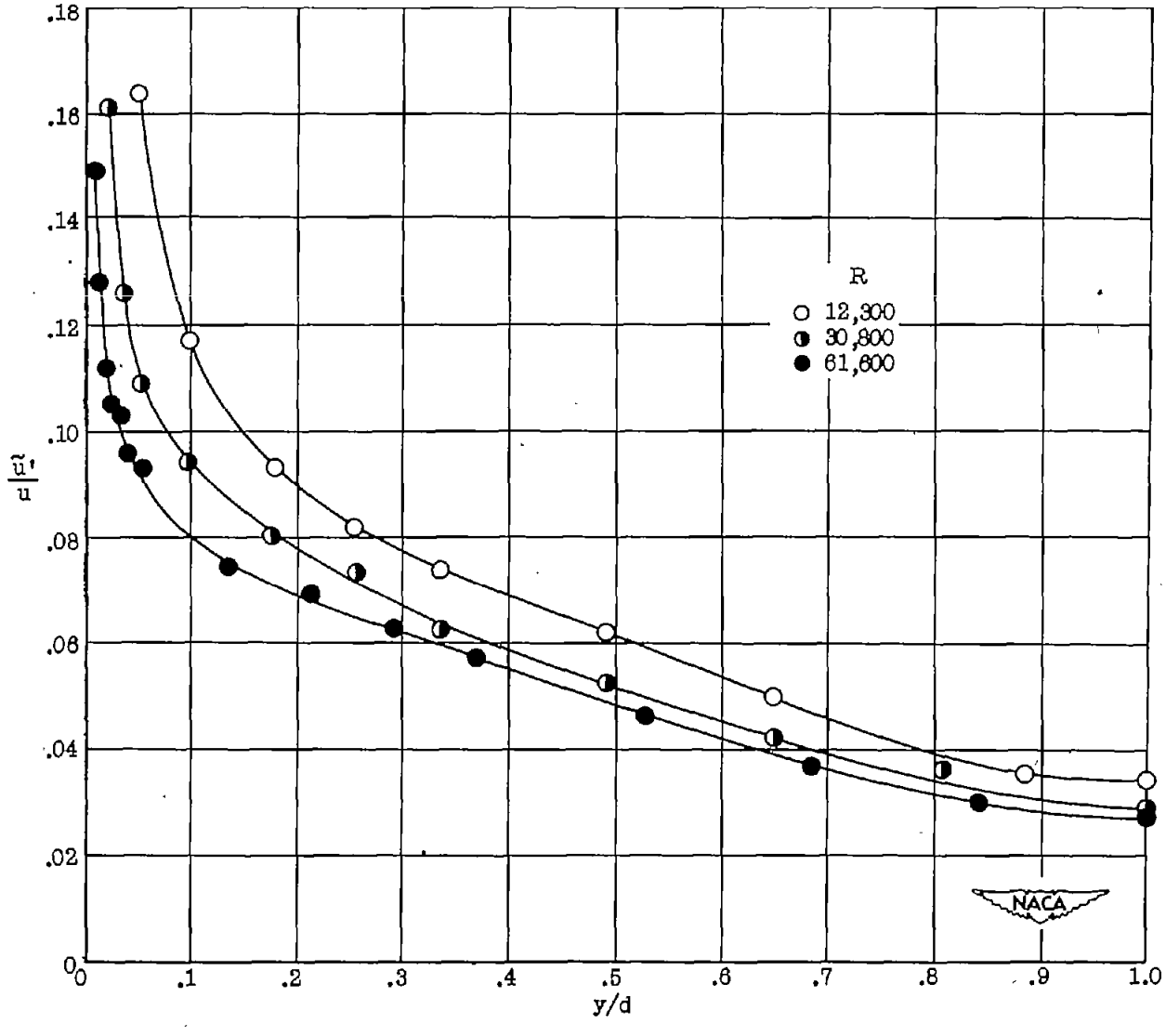

Figure 9.- Velocity fluctuations u' relative to local speeds.

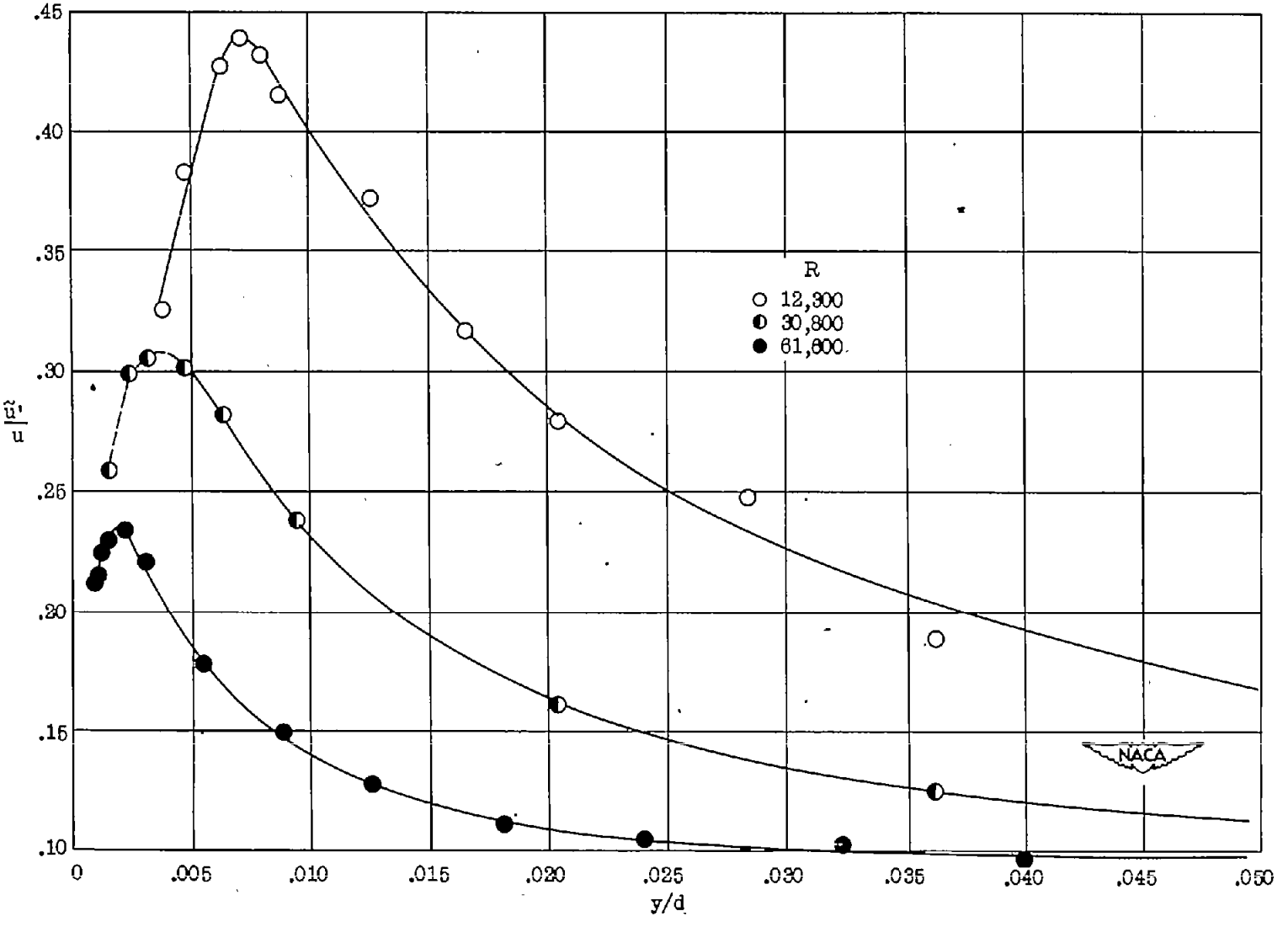

Figure 10.- Velocity fluctuations u' relative to local speeds near wall.

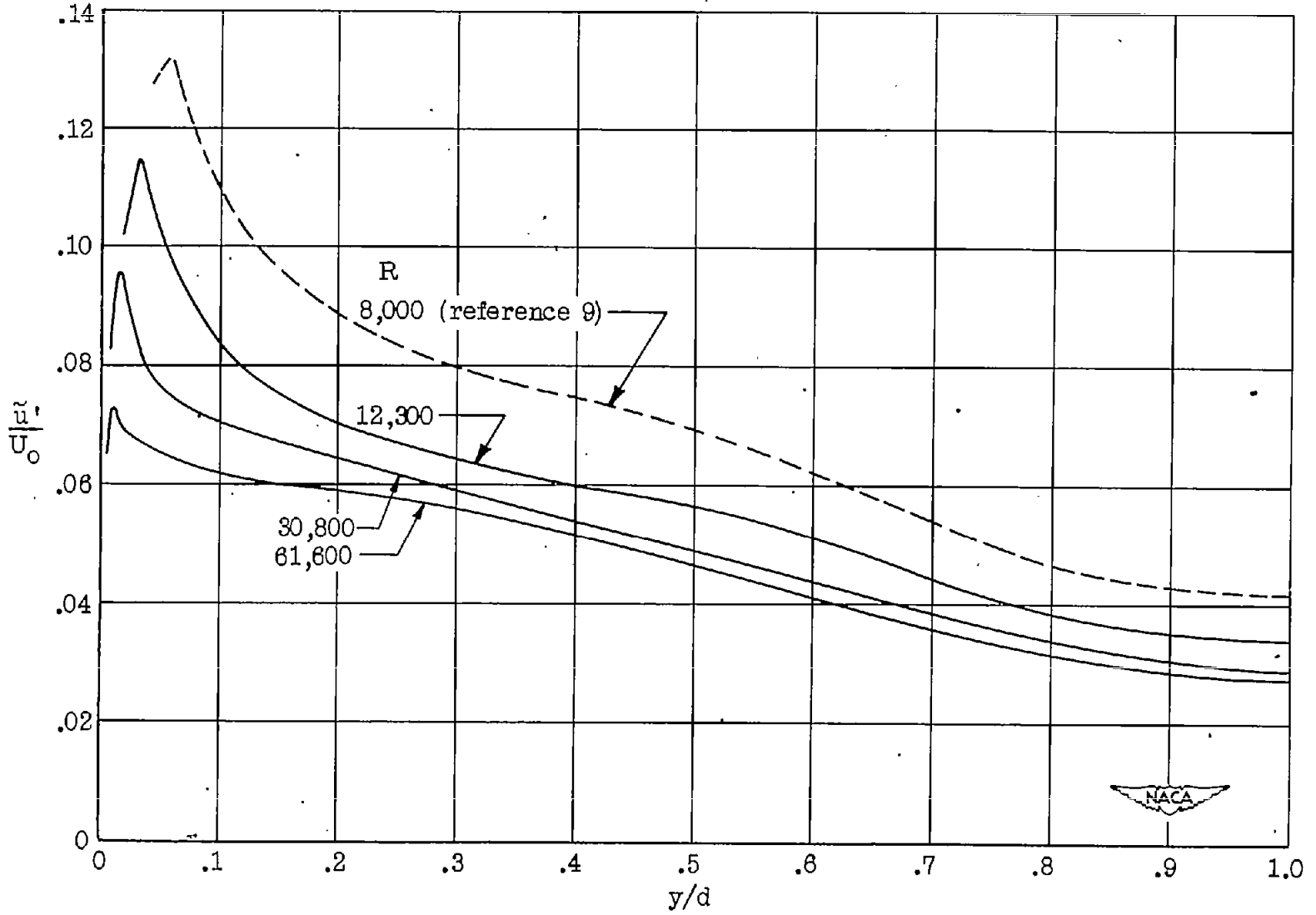

Figure 11.- Velocity fluctuations $\tilde{u}'$.

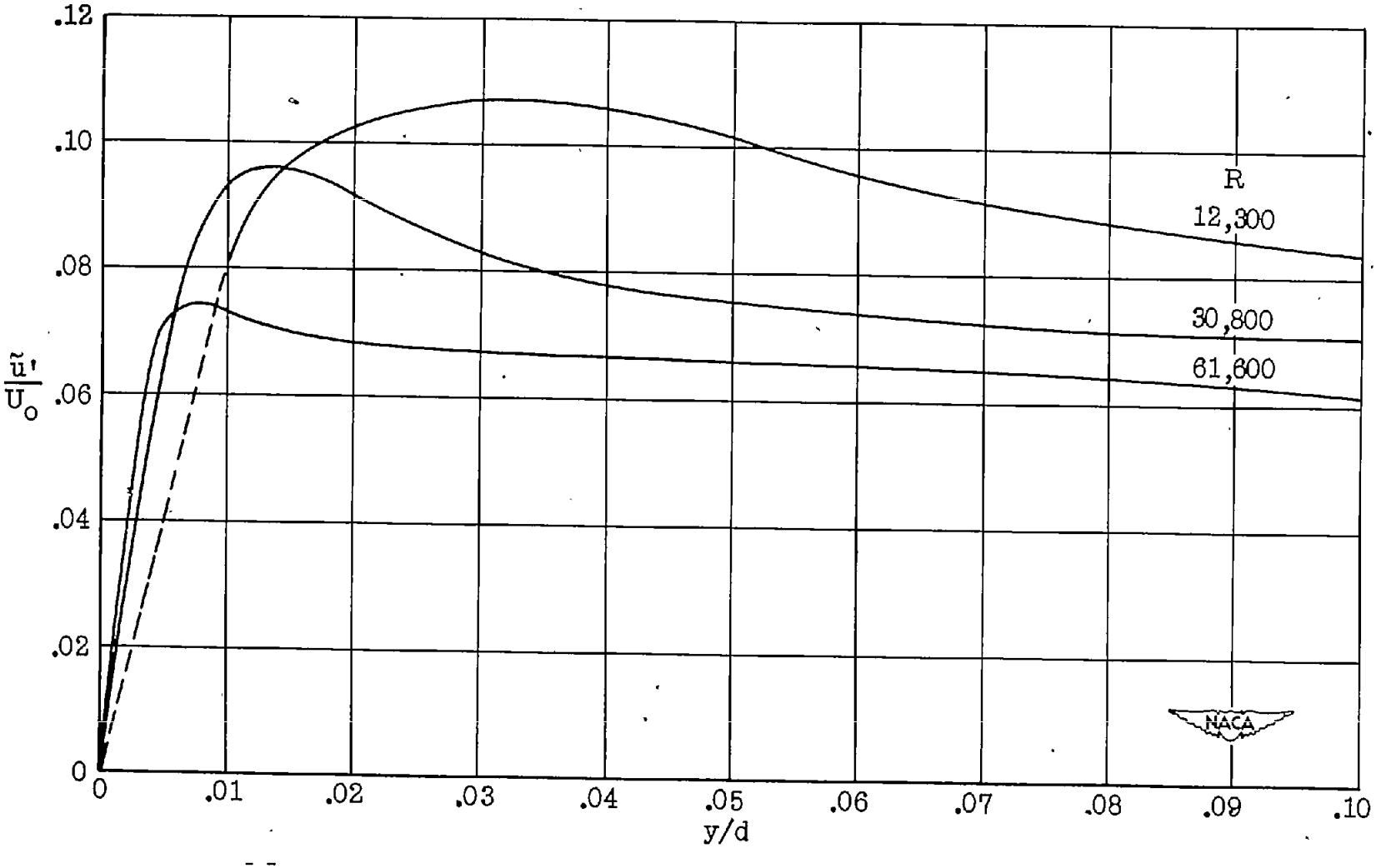

Figure 12.- Velocity fluctuations $\tilde{u}'$ near wall.

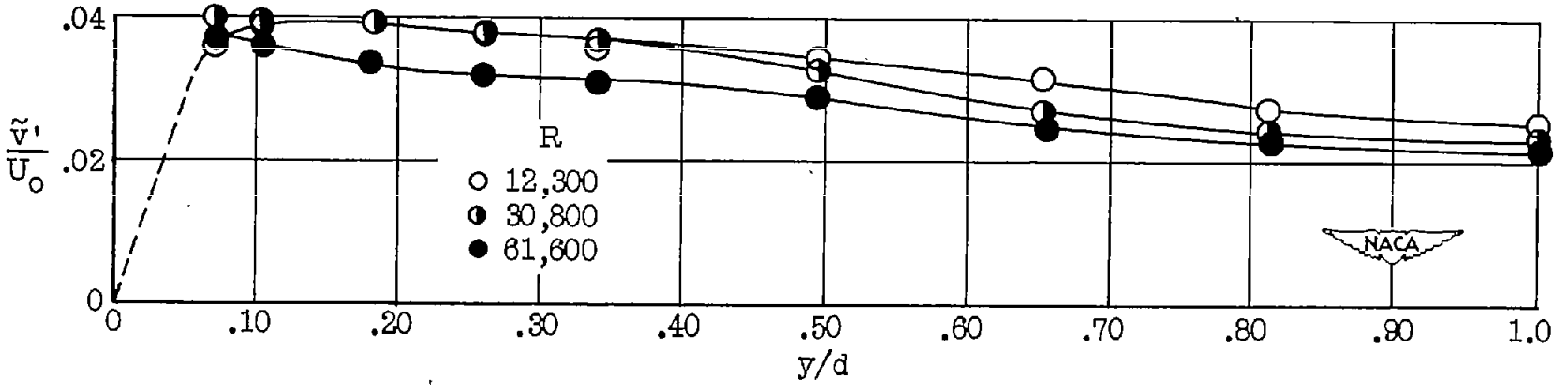

Figure 13.- Distribution of velocity fluctuations $\tilde{v}'$.

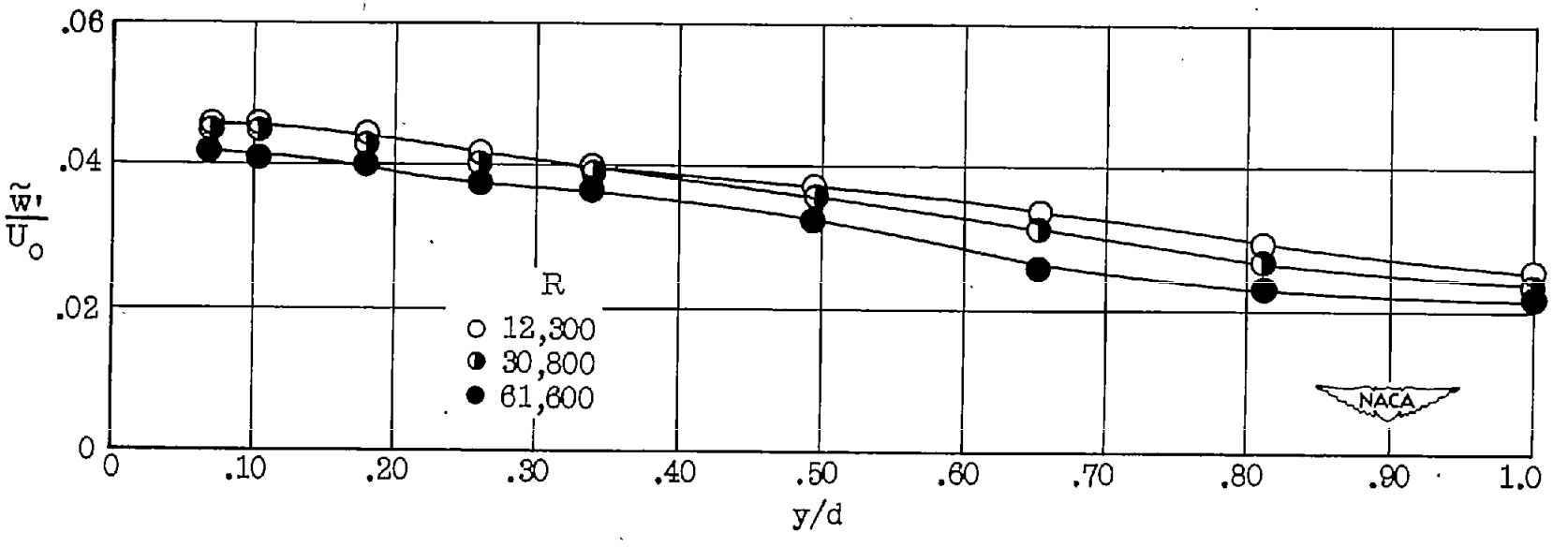

Figure 14.- Distribution of velocity fluctuations $\tilde{w}'$.

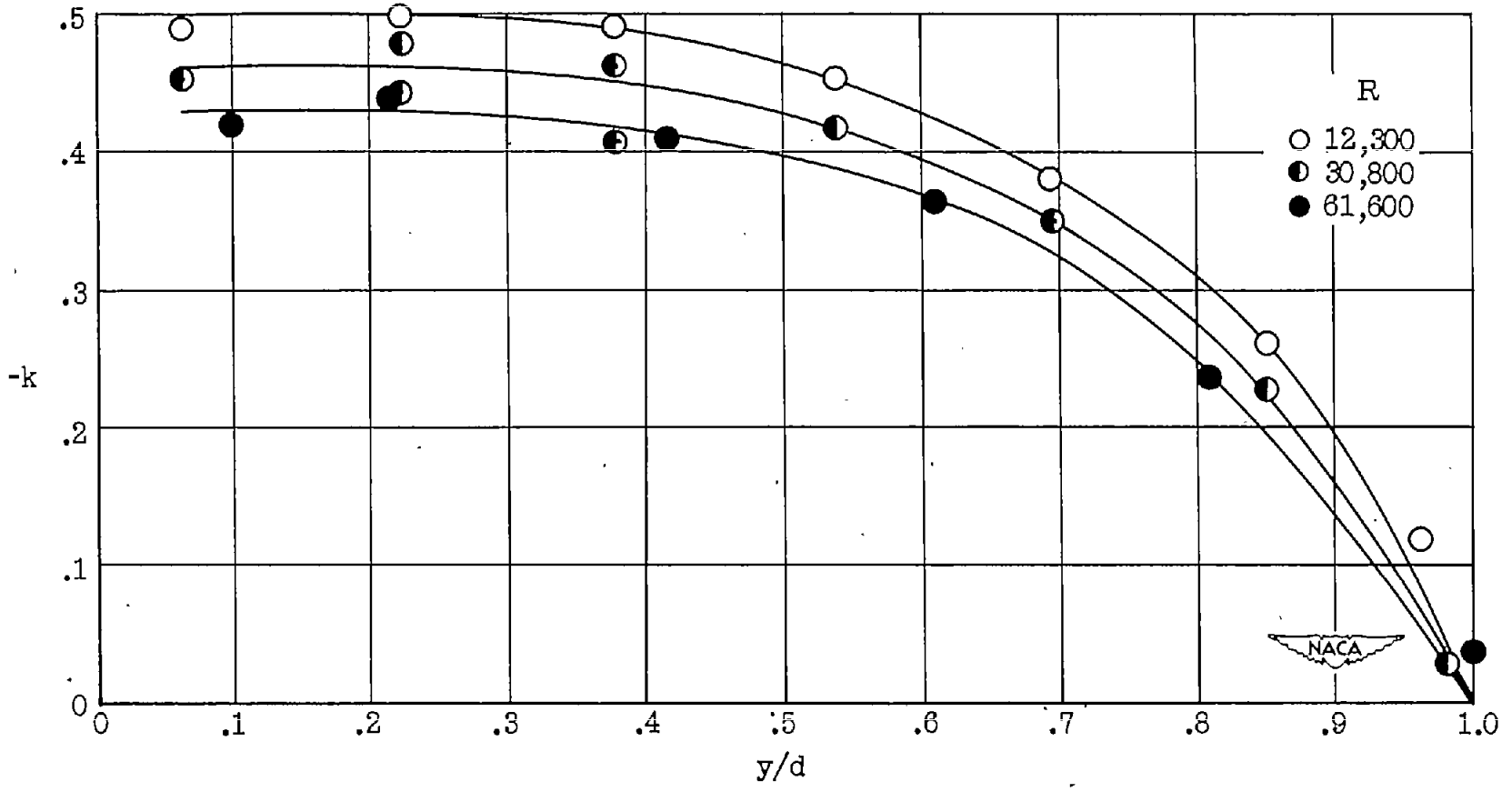

Figure 15.- Correlation-coefficient distribution.

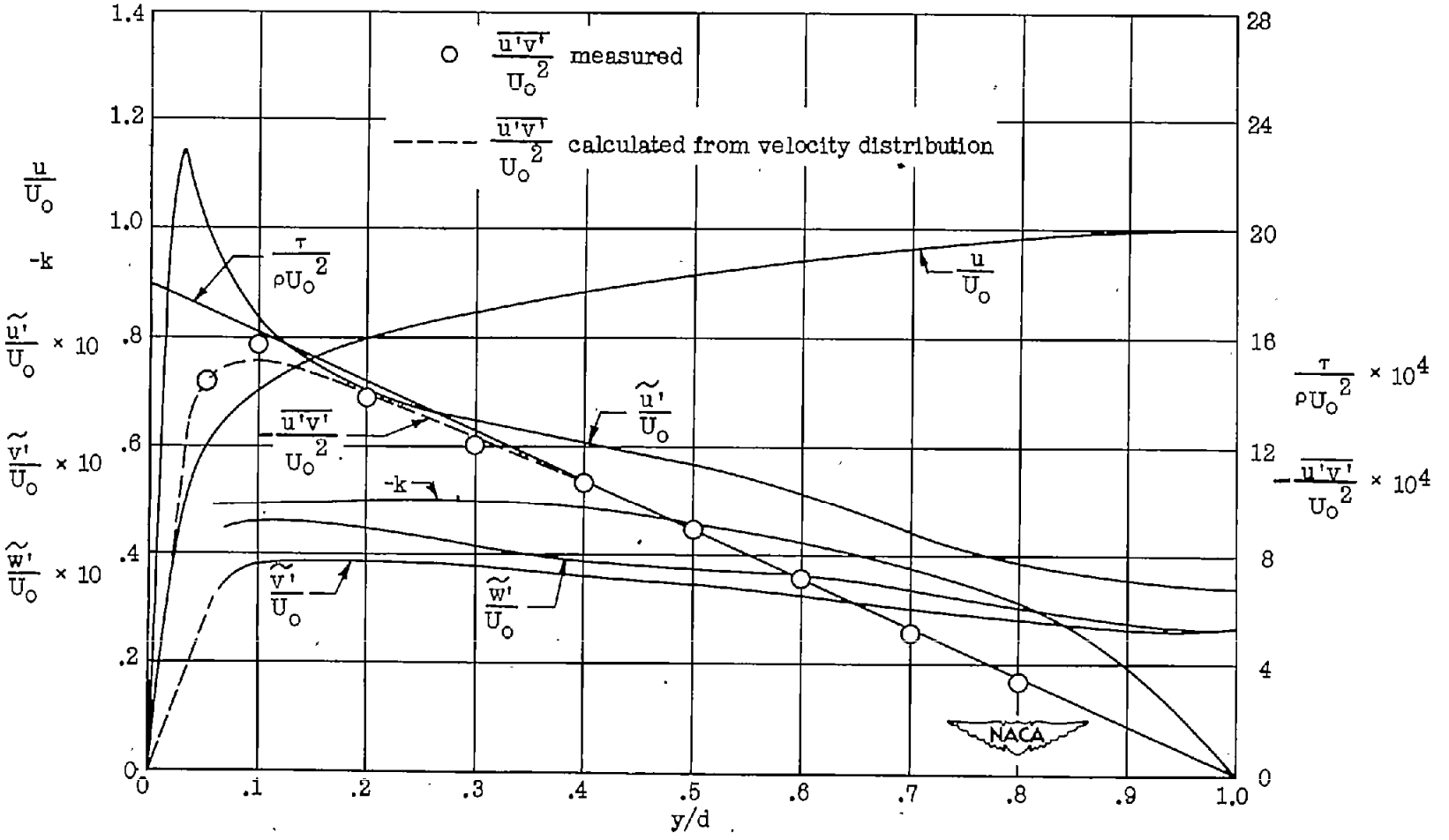

Figure 16.- Distribution of mean and fluctuating quantities. R = 12,300.

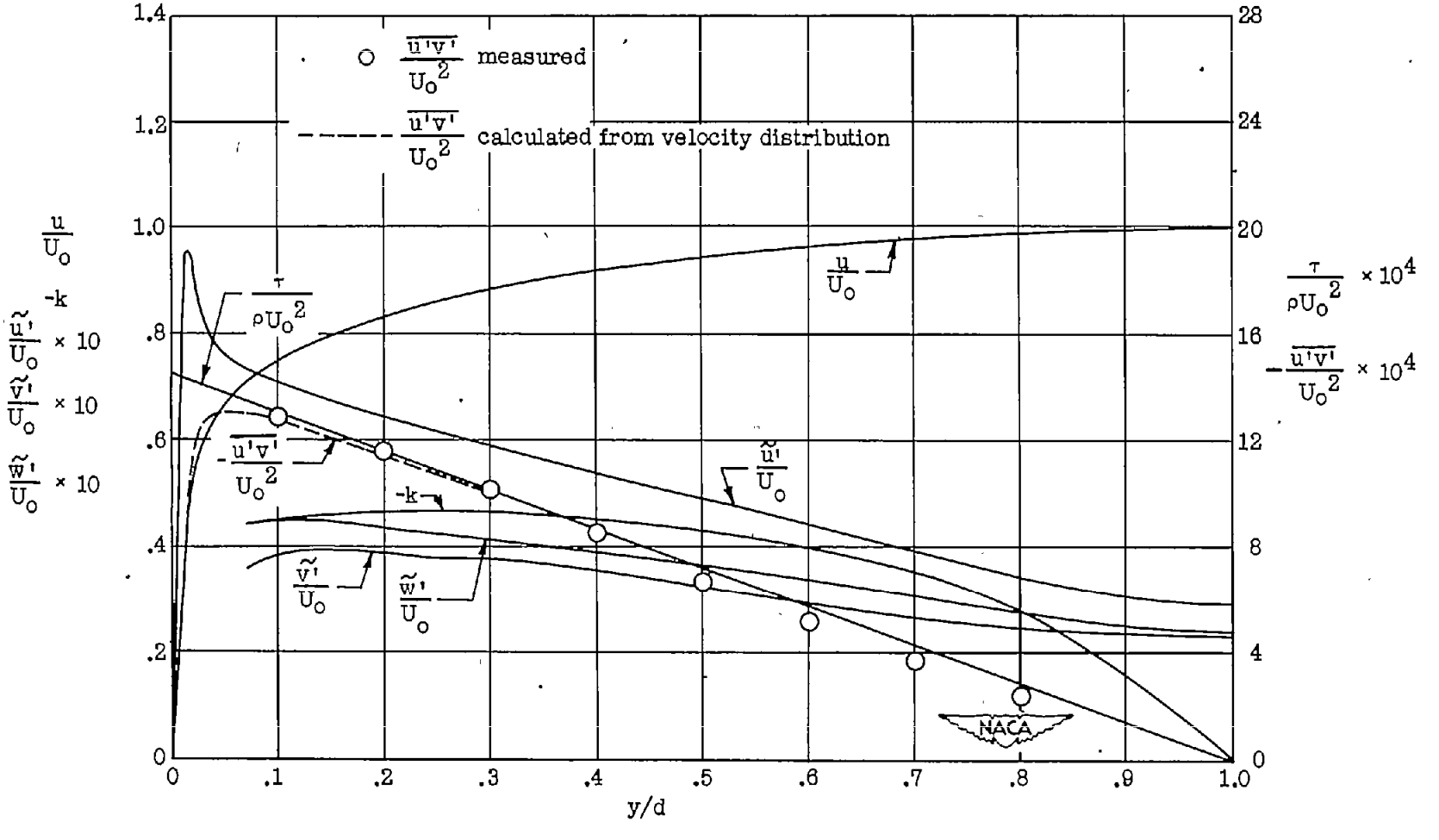

Figure 17.- Distribution of mean and fluctuating quantities. R = 30,800.

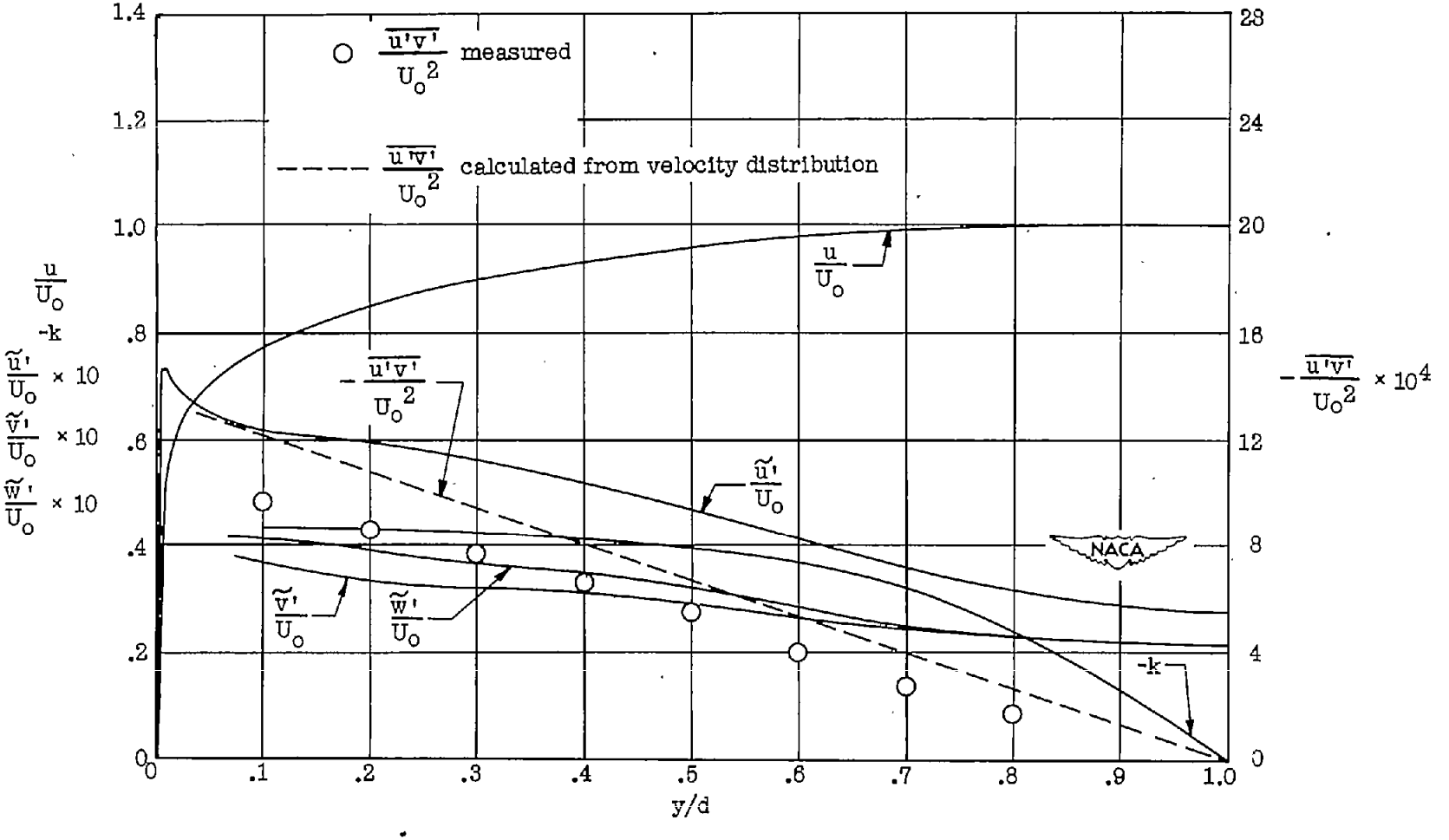

Figure 18.- Distribution of mean and fluctuating quantities. R = 61,600.

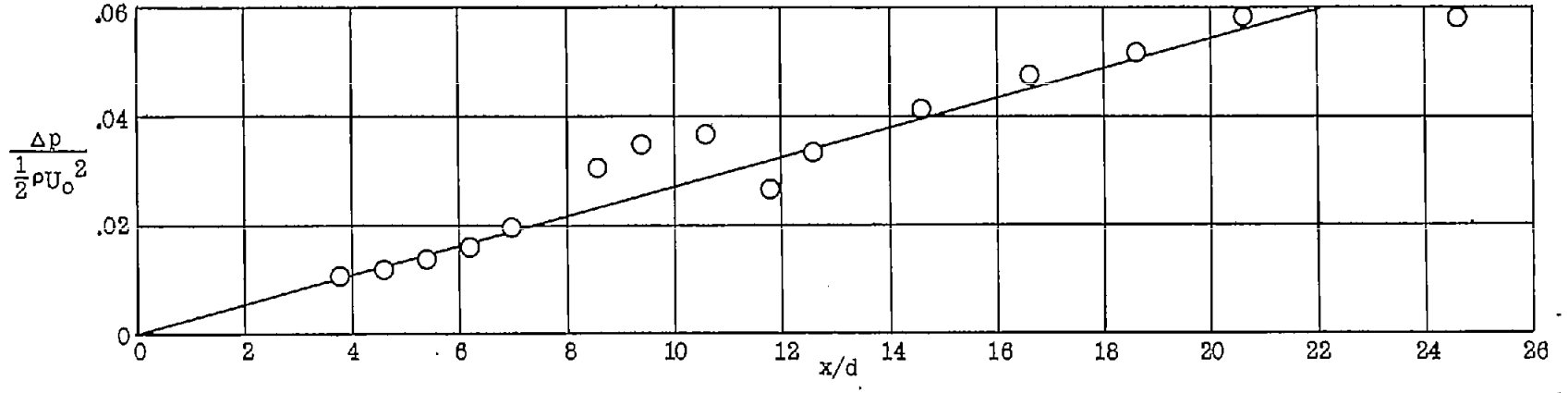

(a) R = 61,600.

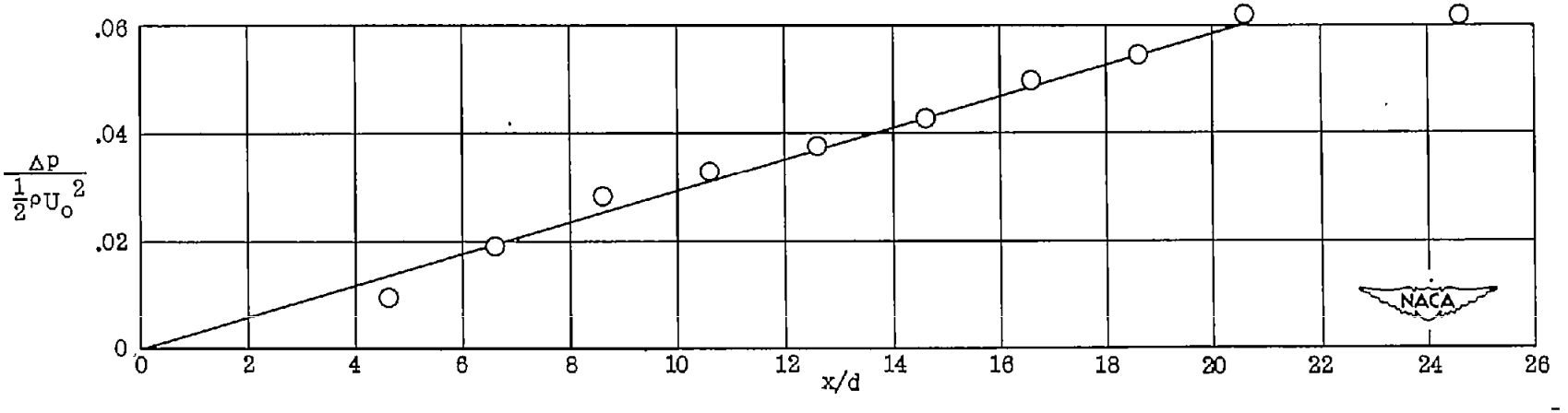

(b) R = 30,800.

Figure 19.- Pressure distribution along channel. Solid lines indicate pressure gradient obtained from measured du/dy.

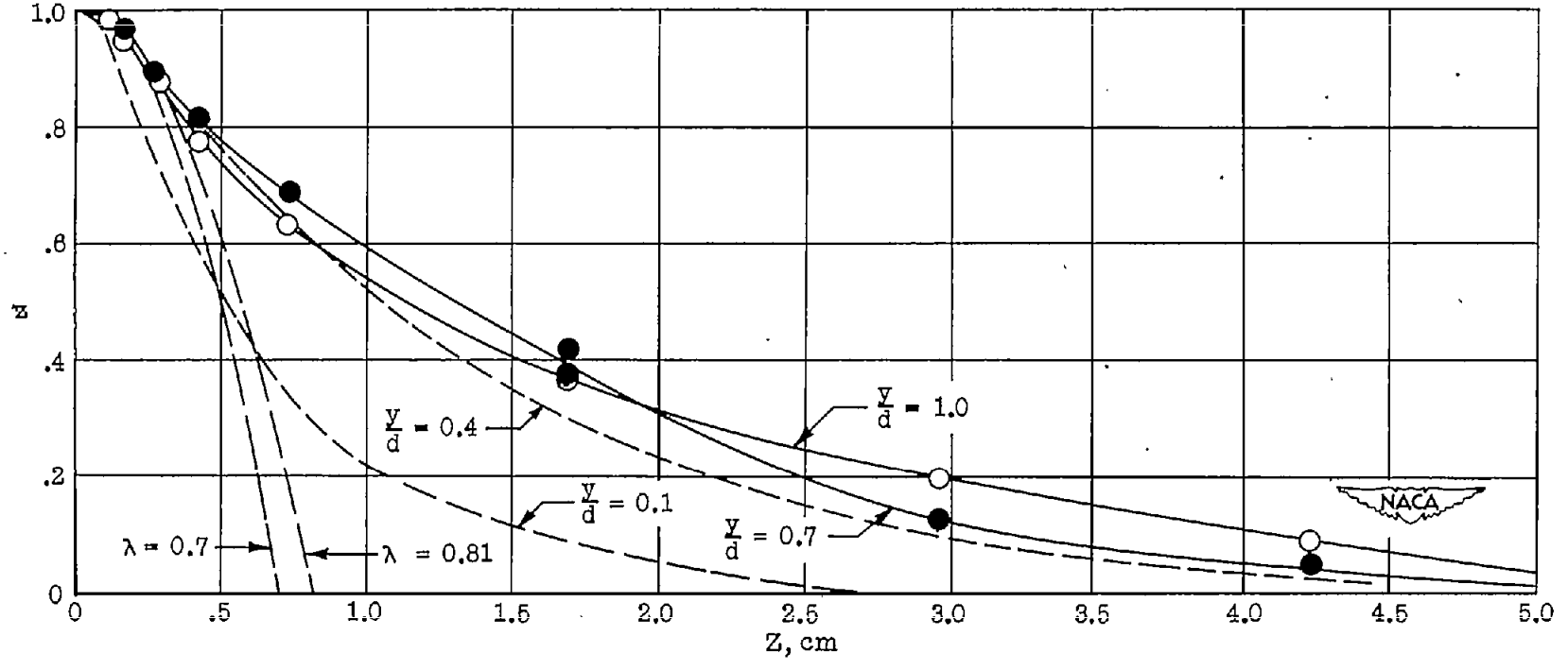

Figure 20.- R_Z-correlation. R = 30,800. At y/d = 1.0, L_Z = 1.65 centimeters, λ_Z = 0.70 centimeter; at y/d = 0.7, L_Z = 1.55 centimeters, λ_Z = 0.81 centimeter.

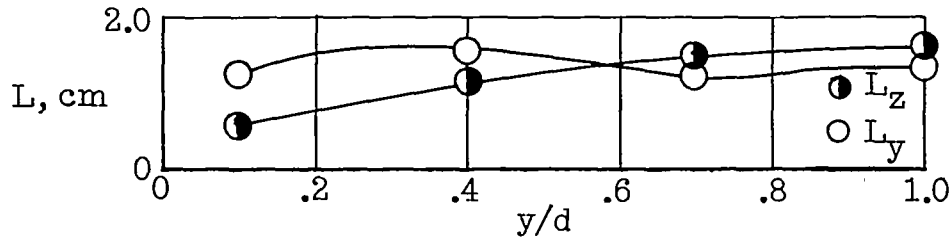

(a) R = 12,300.

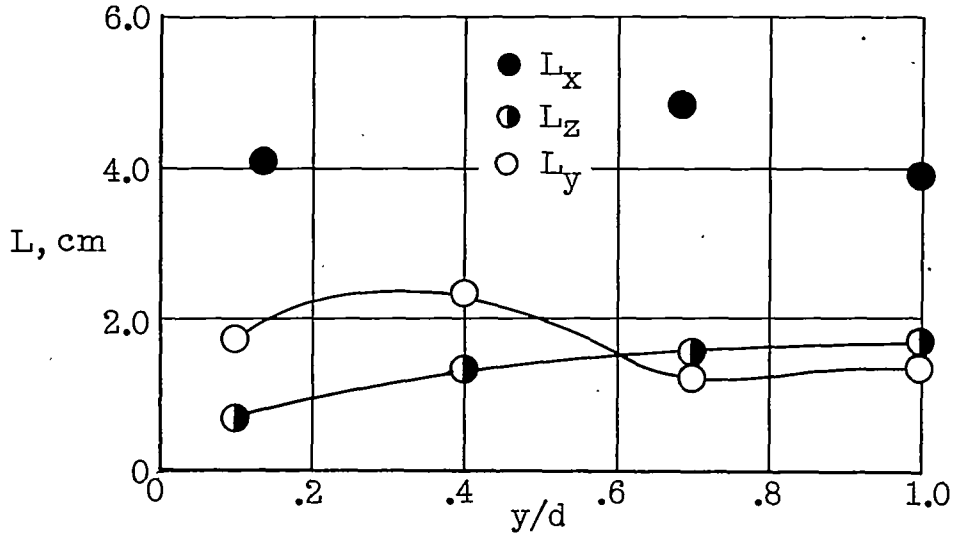

(b) R = 30,800.

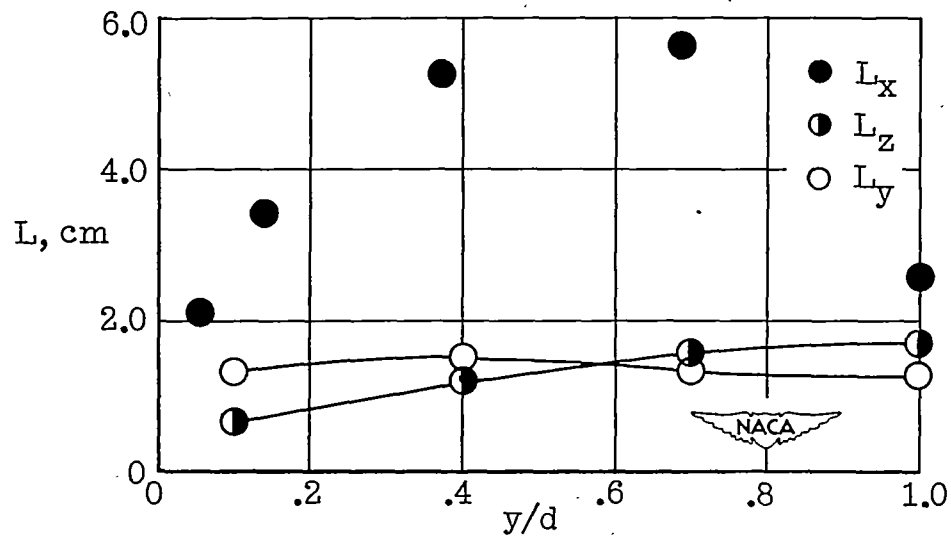

(c) R = 61,600.

Figure 21.- Scale of turbulence distribution.

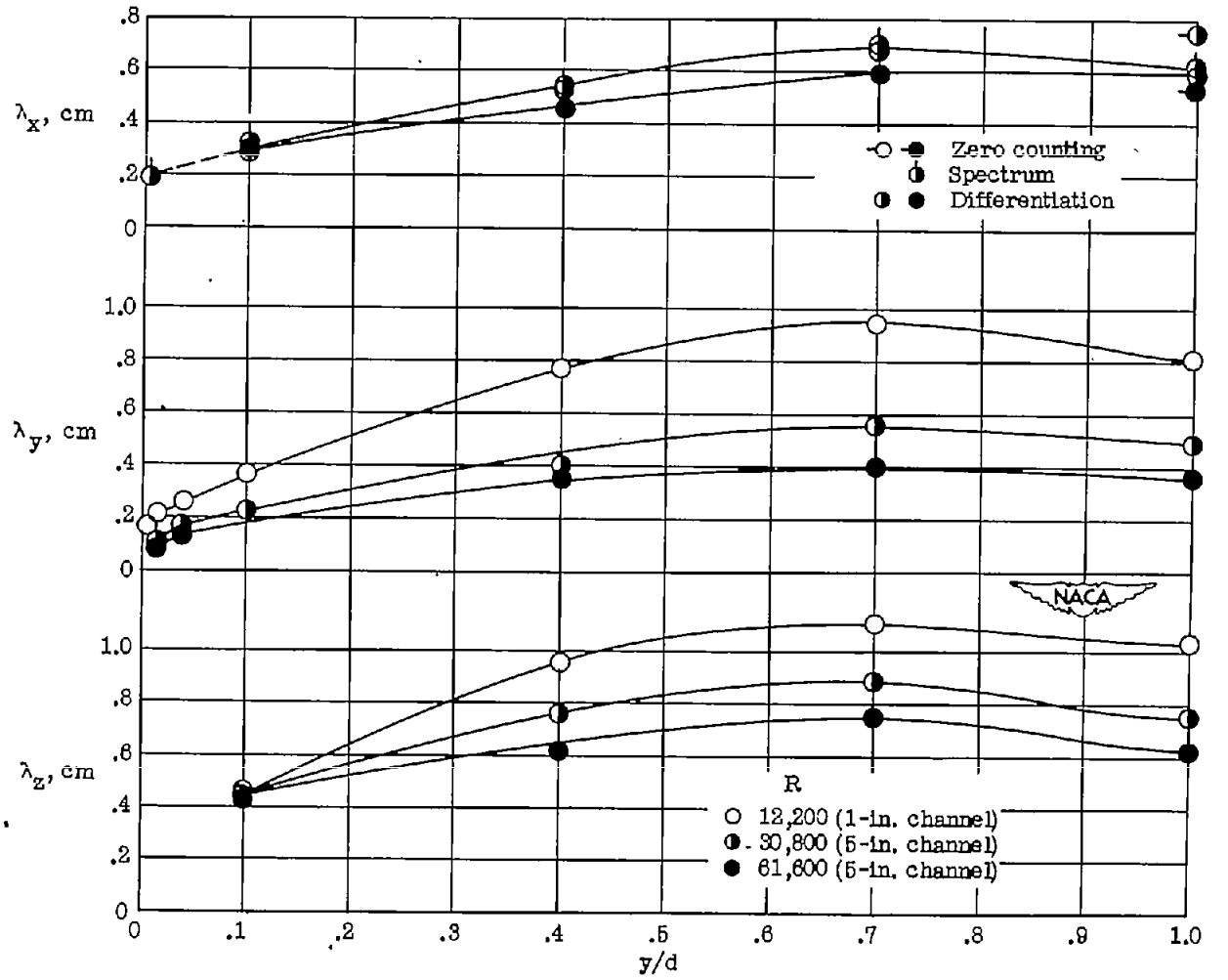

Figure 22.- Microscale measurements. No measurements were made in the 5-inch channel for R = 12,300 because of the inaccuracy due to the large noise-to-signal ratios.

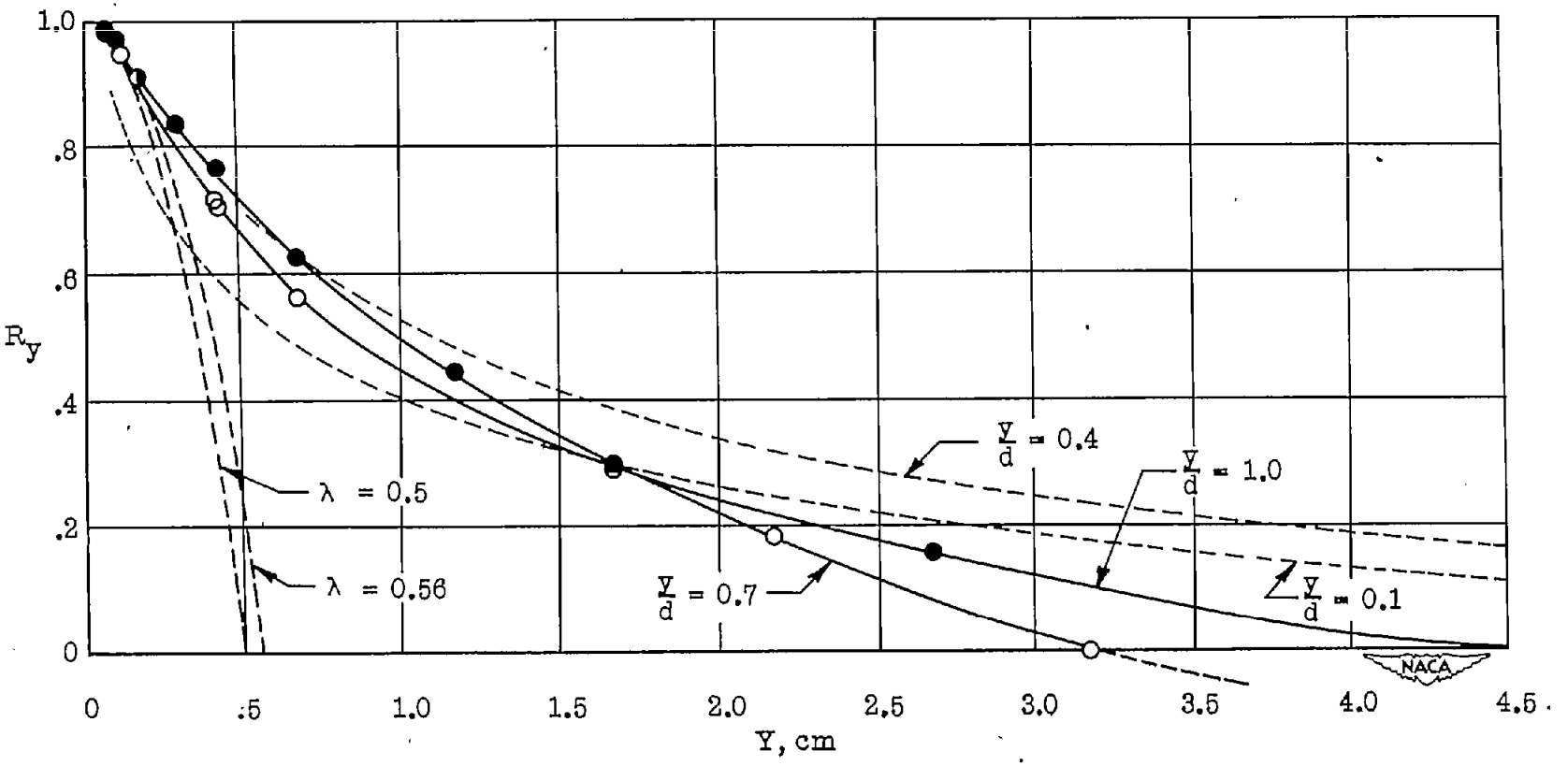

Figure 23.- R_y-correlation. R = 30,800. At y/d = 1.0, L_y = 1.3 centimeters, λ_y = 0.50 centimeter; at y/d = 0.7, L_y = 1.2 centimeters, λ_y = 0.56 centimeter.

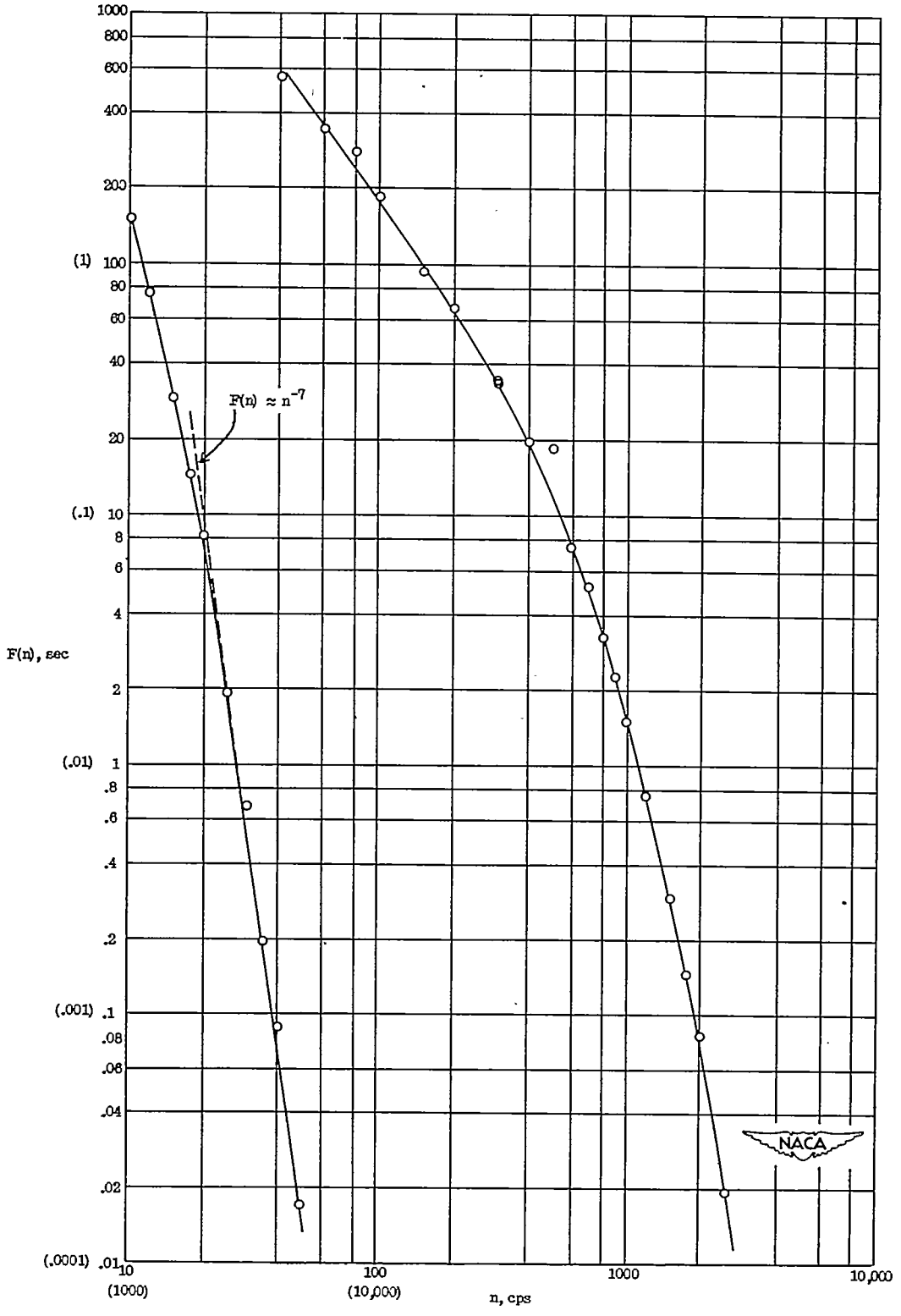

Figure 24.- Frequency spectrum of $\overline{u'^2}$ at channel center. Scale values within parentheses correspond to curve on left.

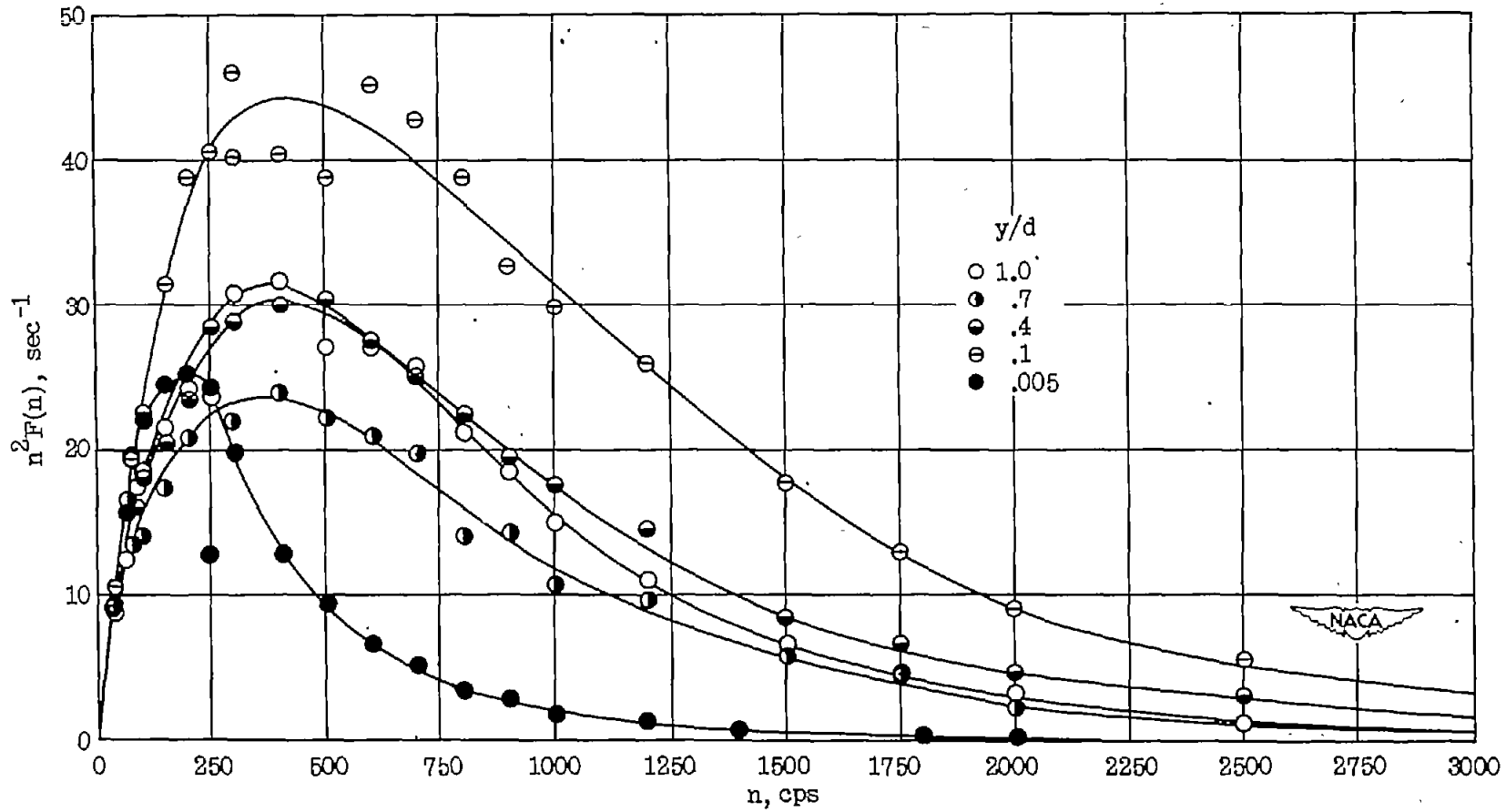

Figure 25.- Spectrum distributions across channel. R = 30,800.

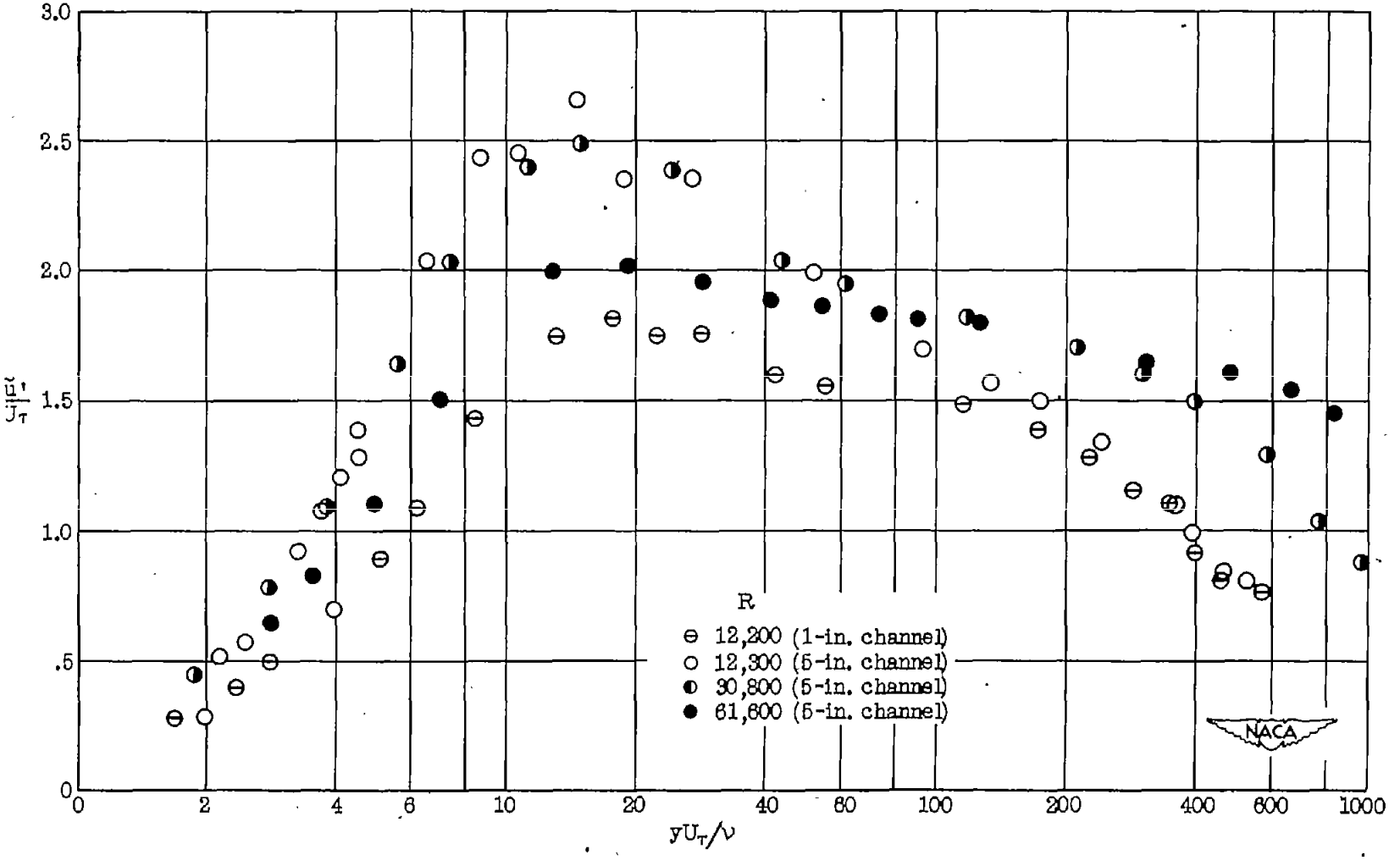

Figure 26.- Logarithmic representation of velocity fluctuations u'.

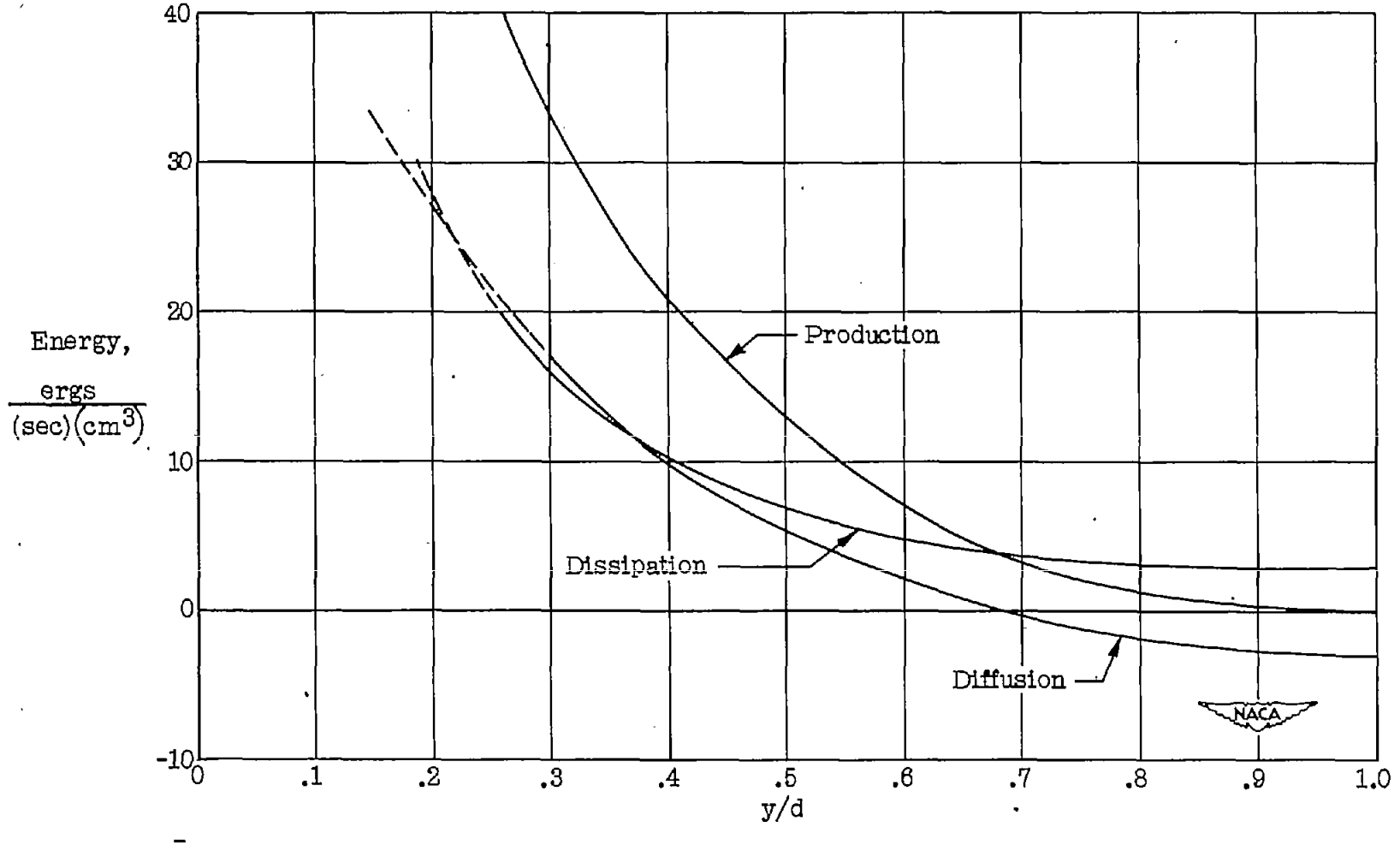

Figure 27.- Turbulent-energy balance in center region of channel. R = 30,800.

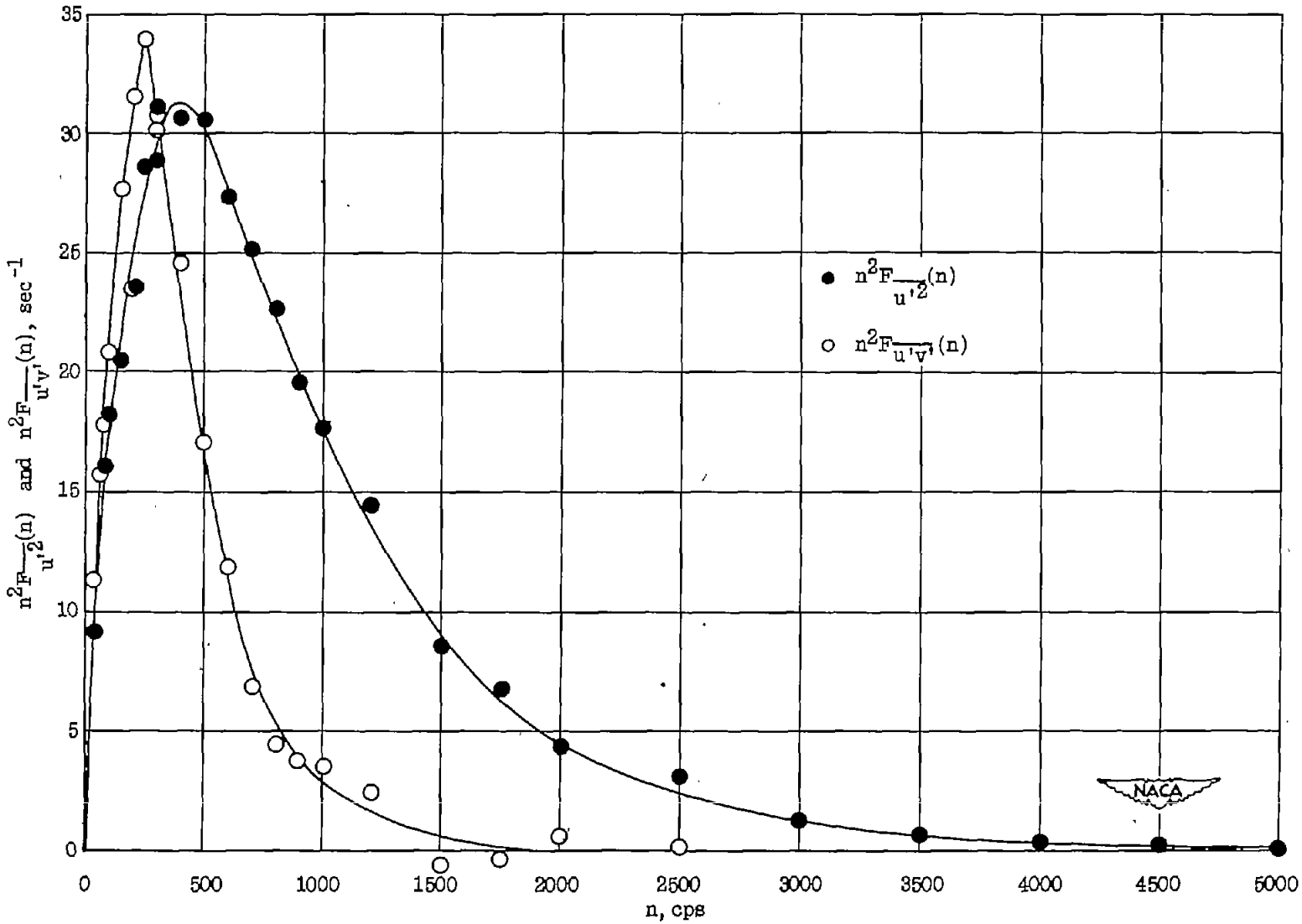

Figure 28.- Comparison of spectrums of $\overline{u'^2}$ and $\overline{u'v'}$ at y/d = 0.4.